Vertical Structure of the Intraseasonal Variability from Contemporary Satellite Data: AIRS, CloudSat, and TRMM

Xianan Jiang

Joint Institute for Regional Earth System Science & Engineering (JIFRESSE) / UCLA

Baijun Tian, and Duane Waliser

Jet Propulsion Laboratory / California Institute of Technology

Outline

I. **Moisture** and **temperature** structures of the MJO: **AIRS** observations versus ERA-Interim

II. **Cloud** structures of the boreal summer ISO: **CloudSat** versus ERA-Interim

III. **Diabatic heating** structures associated with the MJO: **TRMM** observations and reanalysis datasets (ERA-Interim, MERRA, CFS-R).

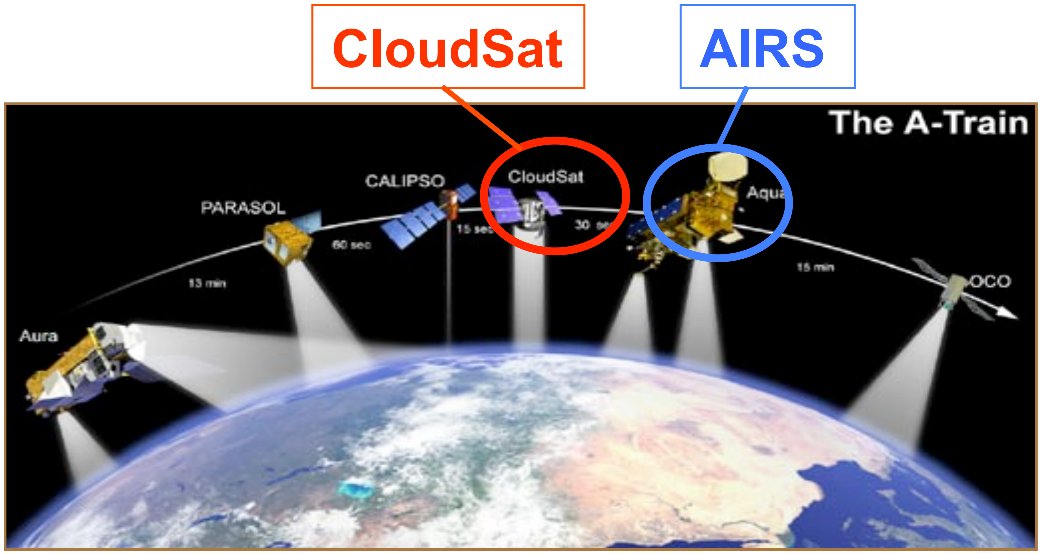

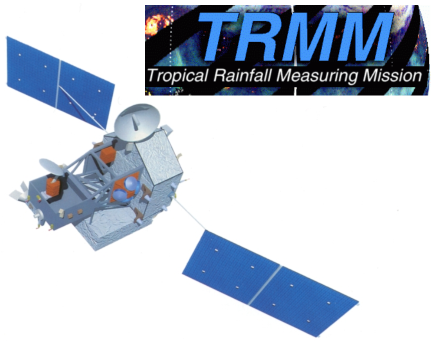

Part I

Vertical moist thermodynamic structure of the MJO in AIRS Observations: An update and a comparison to ECMWF Interim Reanalysis

Analysis by Baijun Tian

Acknowledgements: Eric Fetzer/JPL, and Yuk Yung/Caltech

Tian et al., 2010: Mon Wea Rev, in press.

Tian, B., et al., 2006: Vertical moist thermodynamic structure and spatial-temporal evolution of the MJO in AIRS observations. *J. Atmos. Sci.*, 63, 2462-2485, doi:10.1175/JAS3782.1.

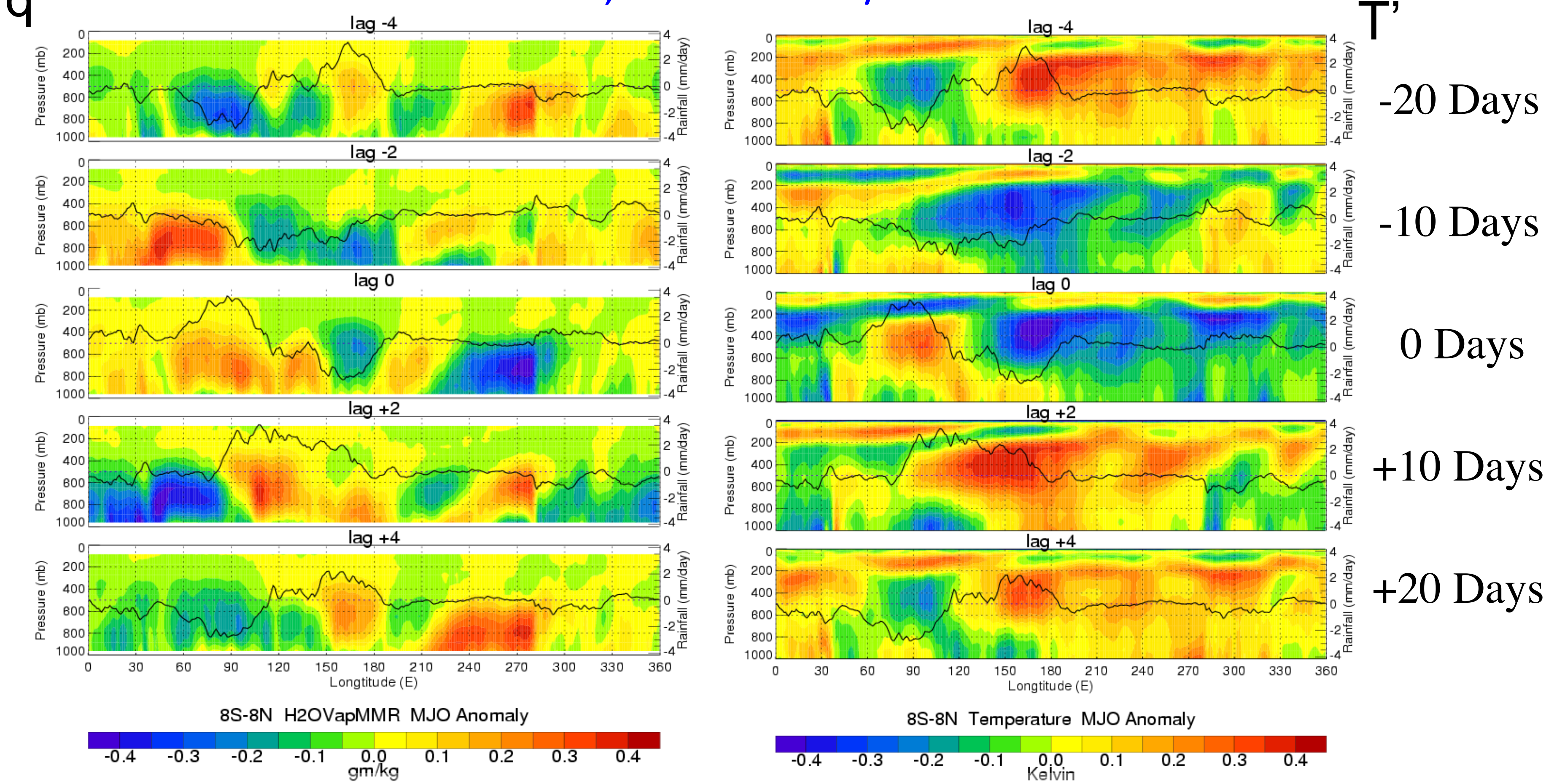

Over the Eastern hemisphere, enhanced (suppressed) convection is generally preceded in both time and space by a low-level warm and moist (cold and dry) anomaly and followed by a low-level cold and dry (warm and moist) anomaly.

Limitation of Tian et al. (2006)

Only 2.5 years (2002-2005, 8 MJO events) of V4 AIRS data were used.

Objective

- Here, we further examine the large-scale vertical moist thermodynamic structure of the MJO using currently available 7-year V5 AIRS data (2002-2009; 17 MJO events) to test its dependence on the AIRS data record lengths, AIRS retrieval versions and MJO event selection and compositing methods employed.
- We also compare the large-scale vertical moist thermo-dynamic structure of the MJO between AIRS and the newer ECMWF Interim reanalysis (ERA-Interim) to evaluate the performance of ERA-Interim in describing the large-scale vertical moist thermodynamic structure of the MJO.

Data

- **TRMM 3B42 Rainfall:**

  40S-40N, 0.25° x 0.25°, 3-hourly, 01/01/1998-05/31/2009.

  Huffman et al. (2007)

- **AIRS Temperature & H2OVapMMR**

  global, 1.0° x 1.0°, V5, L3, 2xdaily, 09/01/2002-06/30/2009.

  24 pressure levels for Temp and 12 layers for H2OVapMMR.

  Chahine et al. (2006)

- **ECMWF Interim Reanalysis Temperature & Specific Humidity**

  global, 1.5° x 1.5°, 4xdaily, 09/01/2002-05/31/2009.

  37 pressure levels from 1000 to 1 hPa for both temperature and specific humidity.

MJO Analysis Methods

(1) Method 1 is the **Extended EOF (EEOF)** method used by Tian et al. (2006).

(2) Method 2 is the **Multivariate EOF (MEOF)** method introduced by Wheeler and Hendon (2004).

EEOF Method

(1) All the data were binned into pentad (5-day) values.

(2) Intraseasonal anomalies were obtained by removing the annual cycle and data filtering through a 30–90-day band pass filter.

(3) Perform an EEOF analysis on band-passed (30-90 day) rainfall data (e.g., TRMM, CMAP) over the tropical Indian Ocean and western Pacific.

(4) Identify MJO events from the PC time series of 1st EEOF mode.

(5) Composite MJO events in band-passed rainfall and target quantity (e.g., temperature, moisture, ozone, aerosols).

Tian et al. (2006)

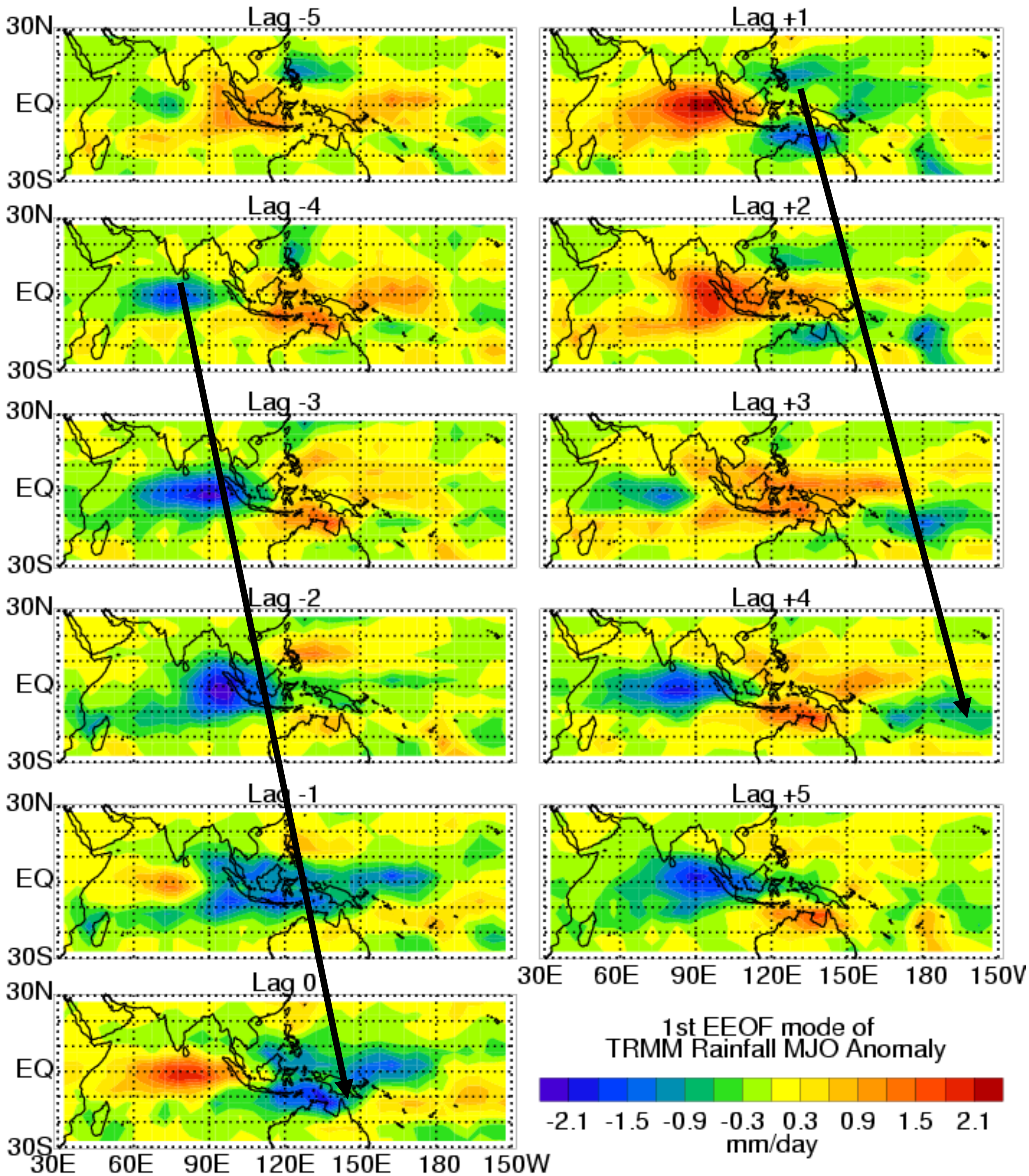

Spatial-temporal Pattern of the 1st EEOF Mode of Rainfall MJO Anomaly

1998-2005
Tian et al. (2006)

Amplitude Time Series of the 1st EEOF Mode of Rainfall MJO Anomaly

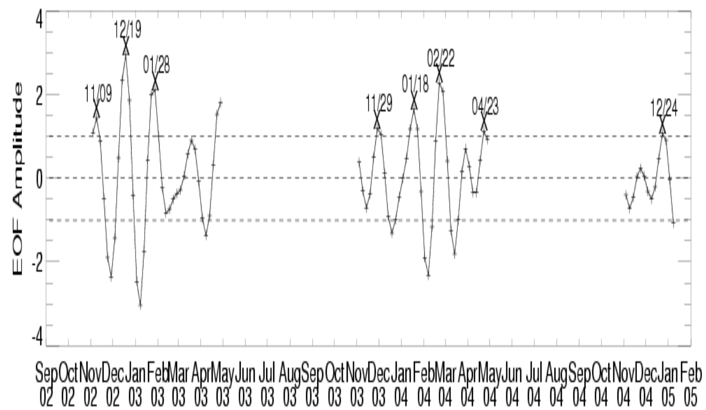

The x indicates the dates of selected MJO events for 2002-2005 (8)

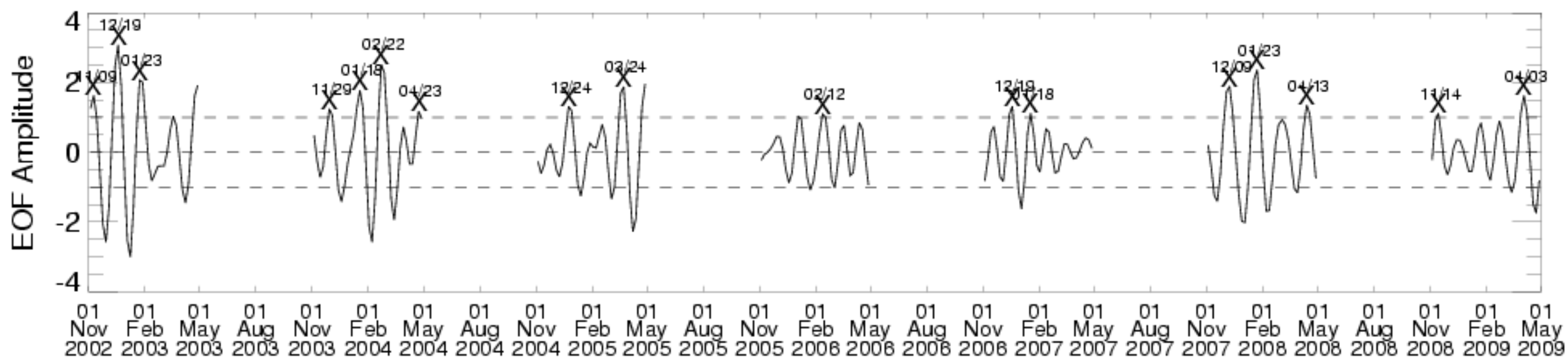

The x indicates the dates of selected MJO events for 2002-2009 (17)

Comparison of 2.5- and 7-yr

T’

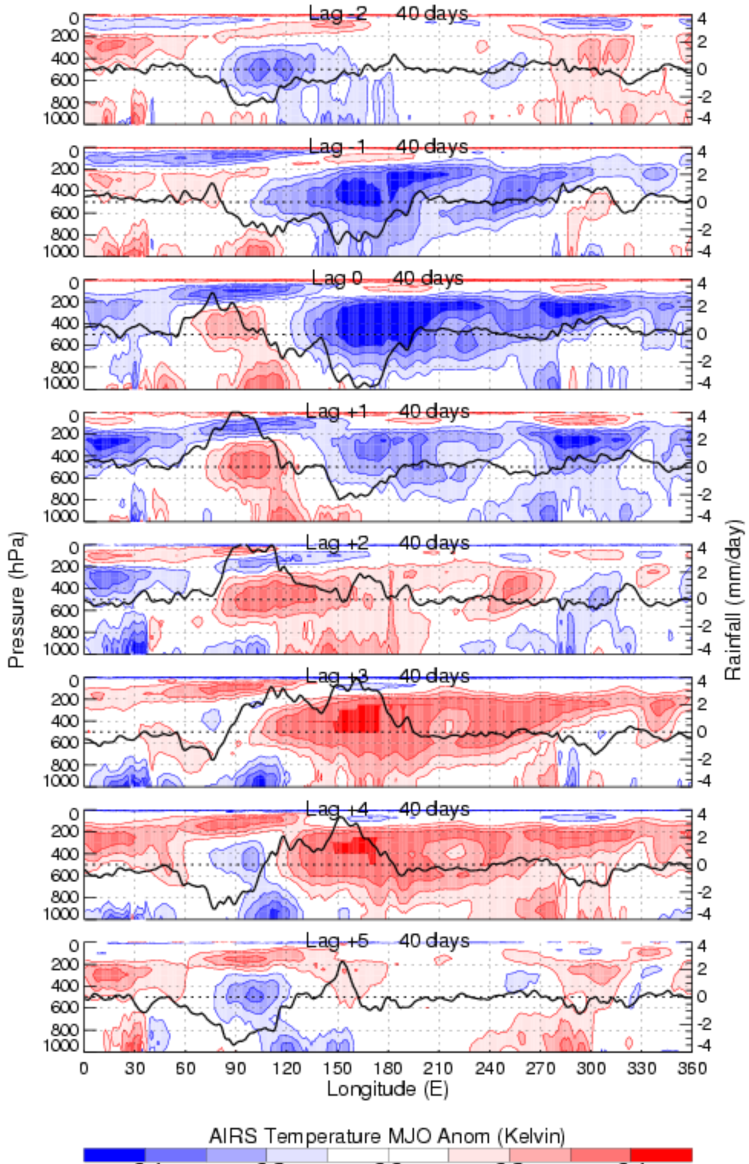

2.5-yr V5 AIRS data & EEOF method

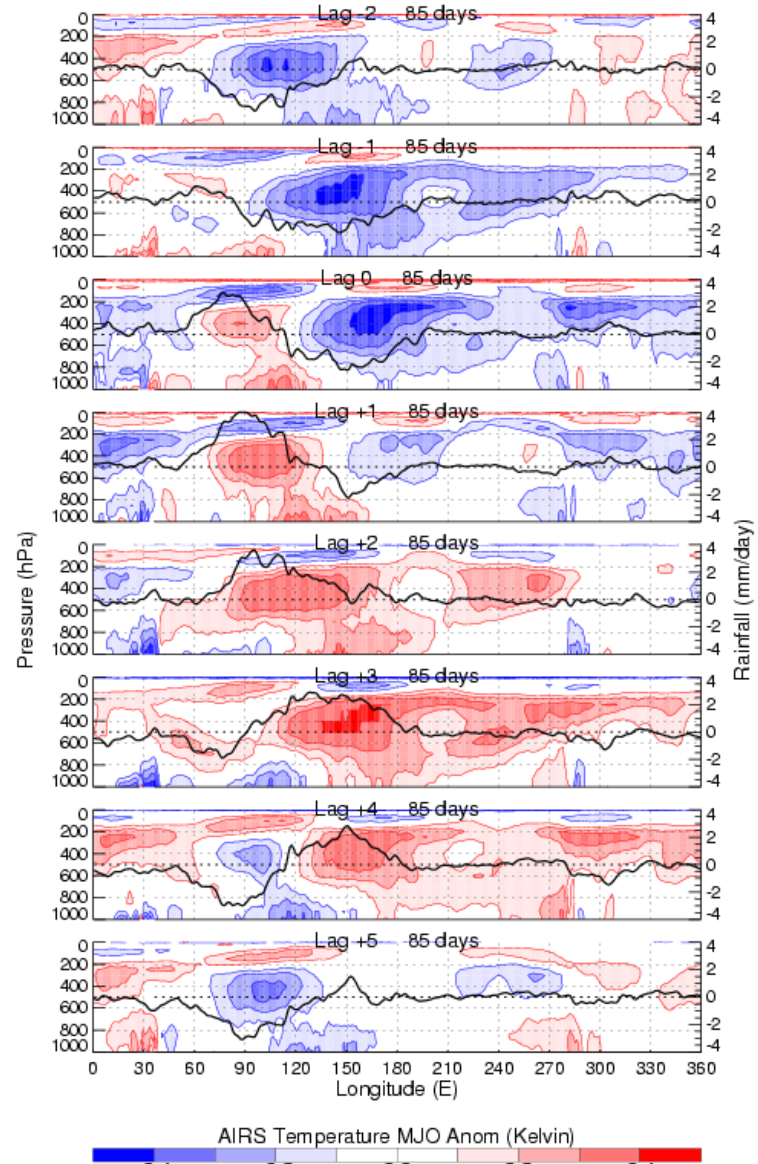

7-yr V5 AIRS data & EEOF method

Comparison of 2.5- and 7-yr

q'

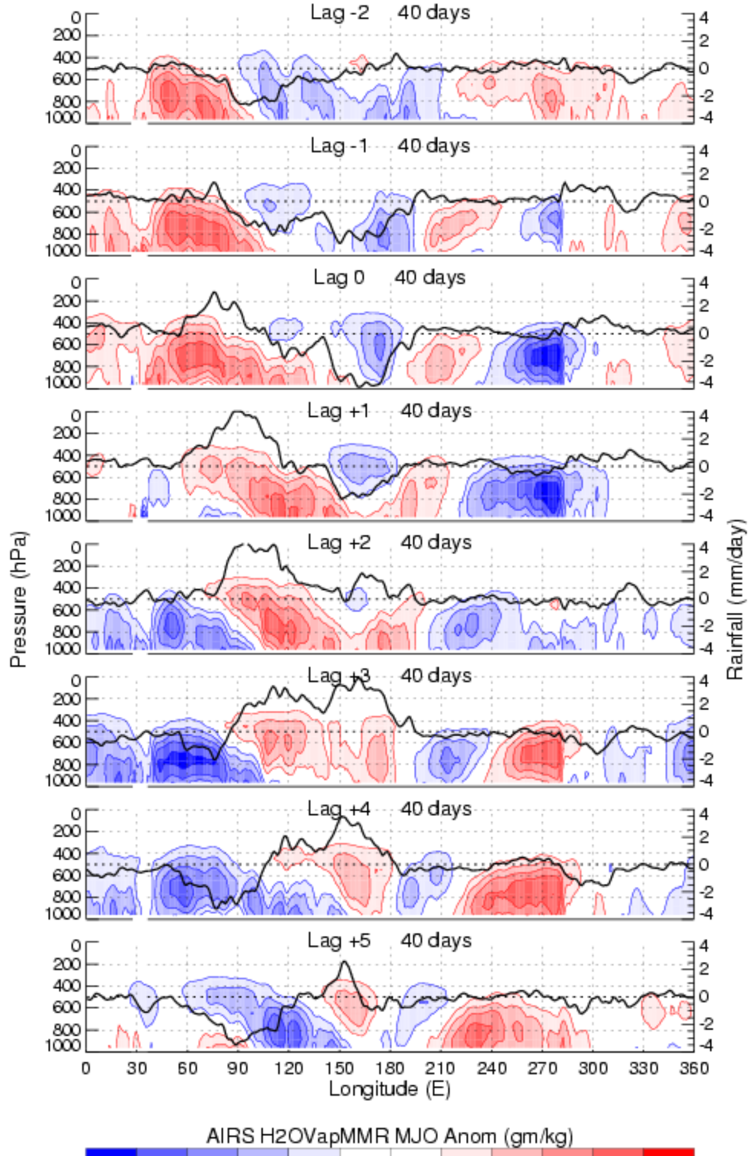

2.5-yr V5 AIRS data & EEOF method

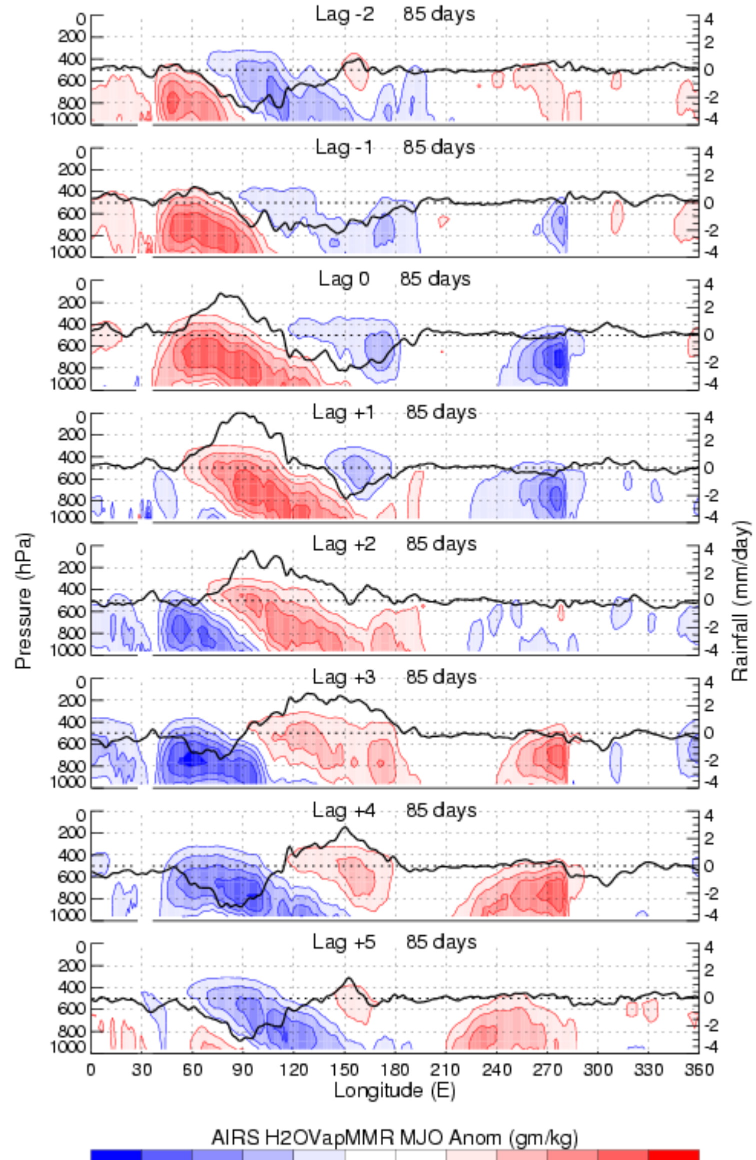

7-yr V5 AIRS data & EEOF method

Comparison of EEOF and MEOF

T'

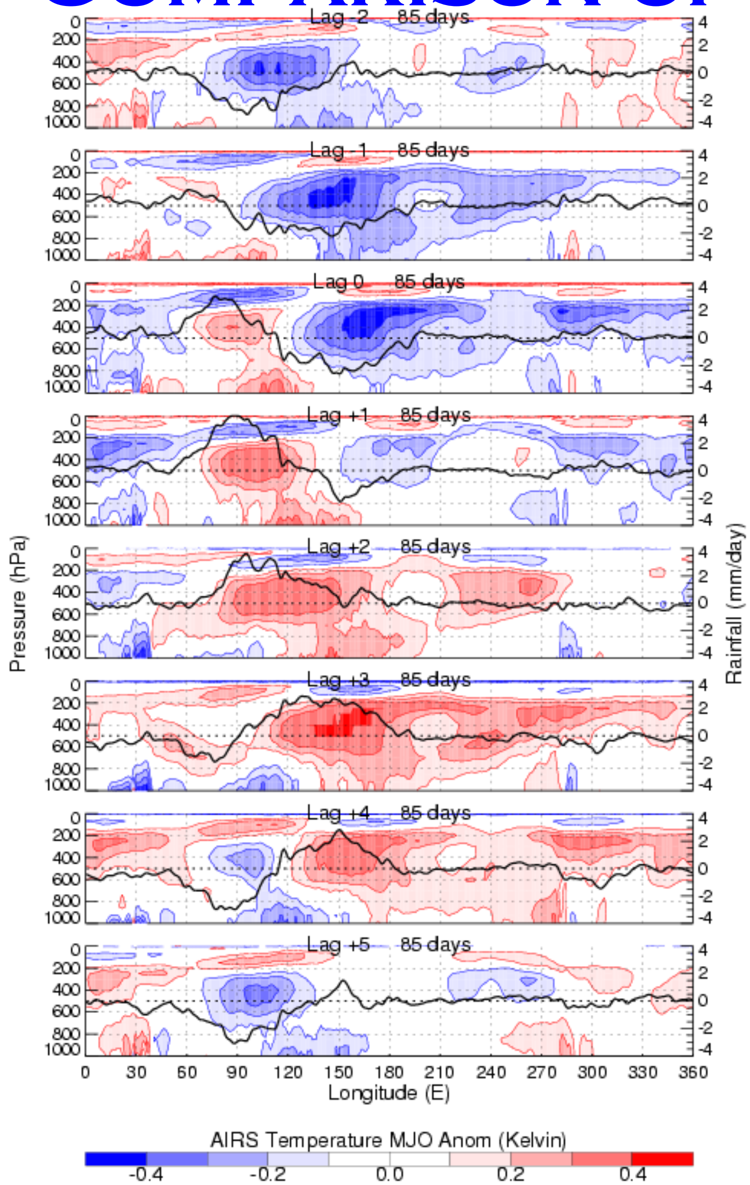

7-yr V5 AIRS data & EEOF method

7-yr V5 AIRS data & MEOF method

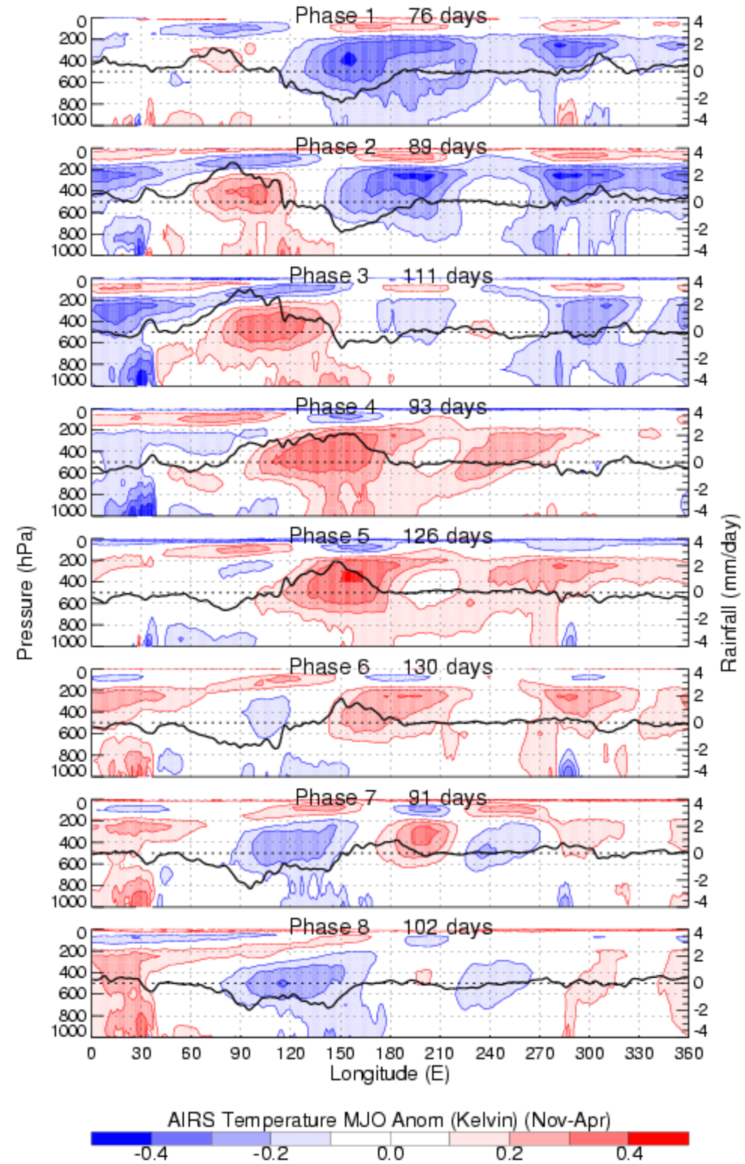

Comparison of EEOF and MEOF

q'

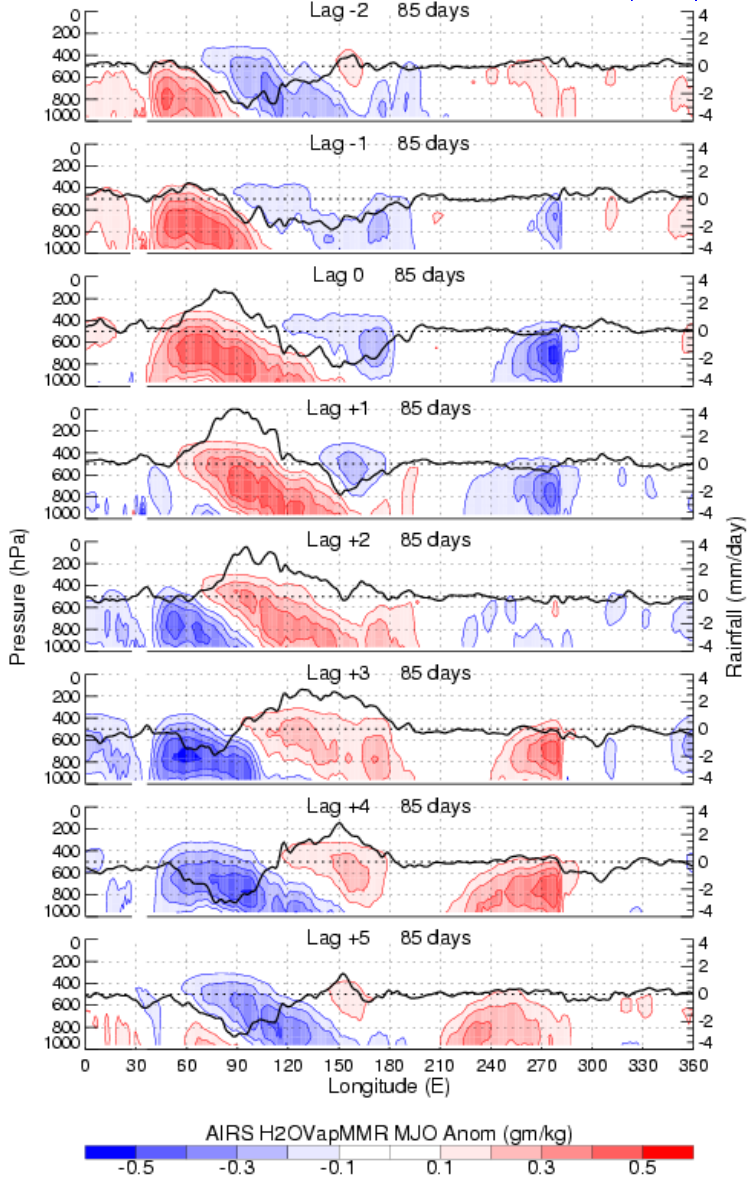

7-yr V5 AIRS data & EEOF method

7-yr V5 AIRS data & MEOF method

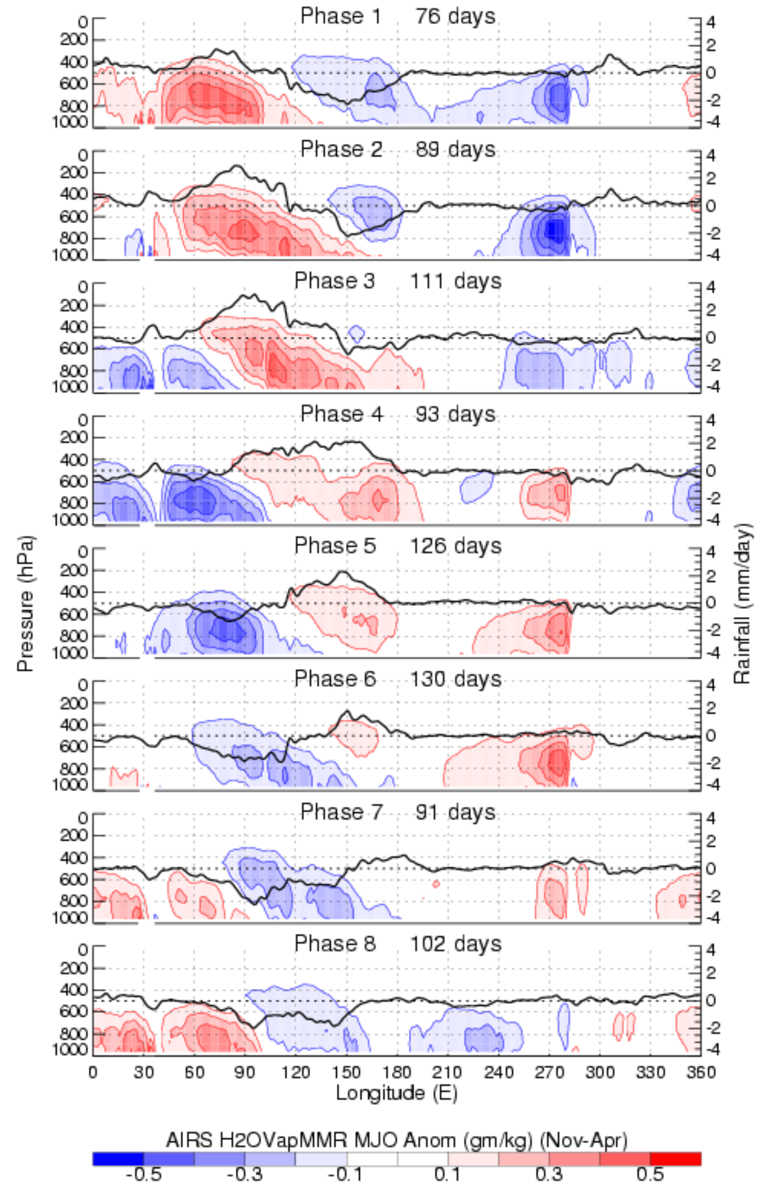

Comparison of AIRS and ERA-Interim

T'

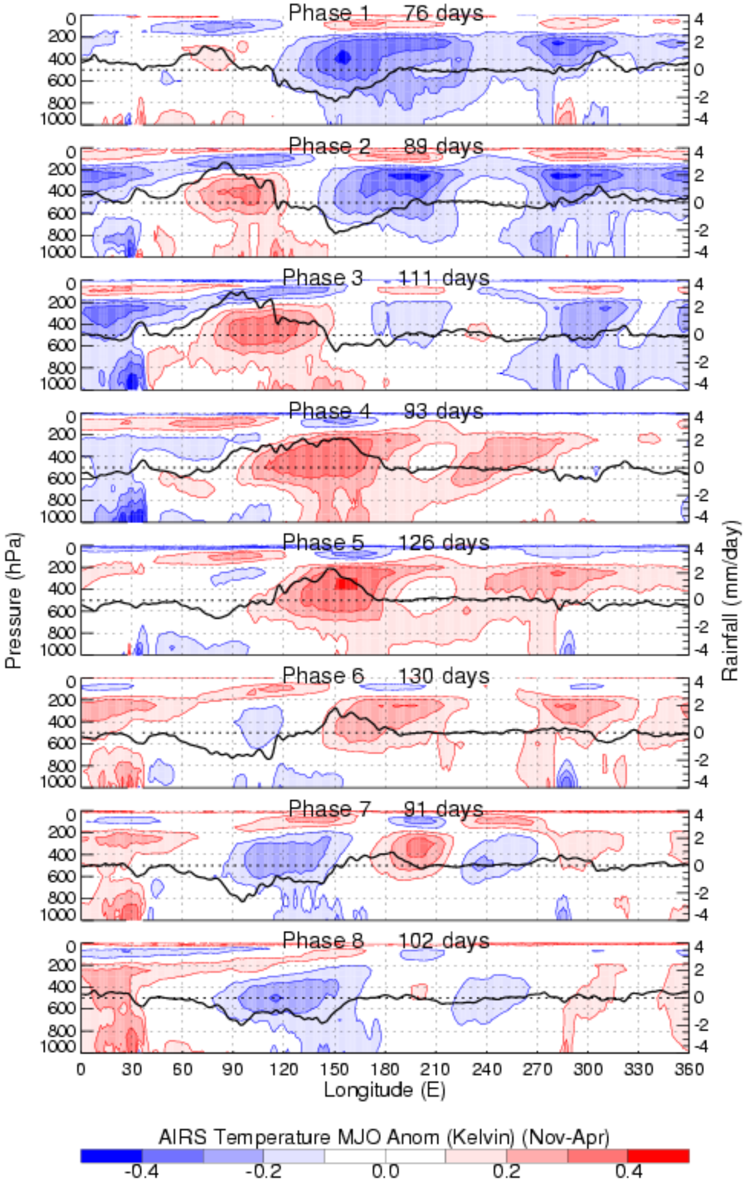

7-yr V5 AIRS data & MEOF method

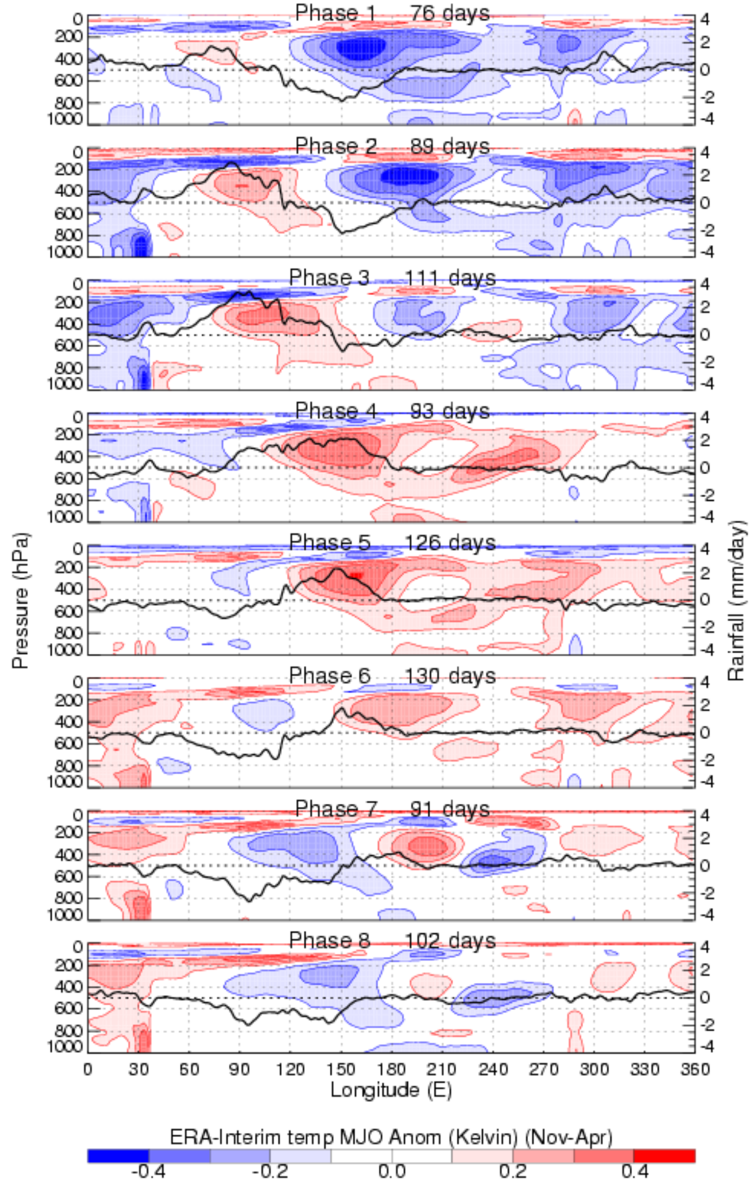

7-yr ERA data & MEOF method

Comparison of AIRS and ERA-Interim

q’

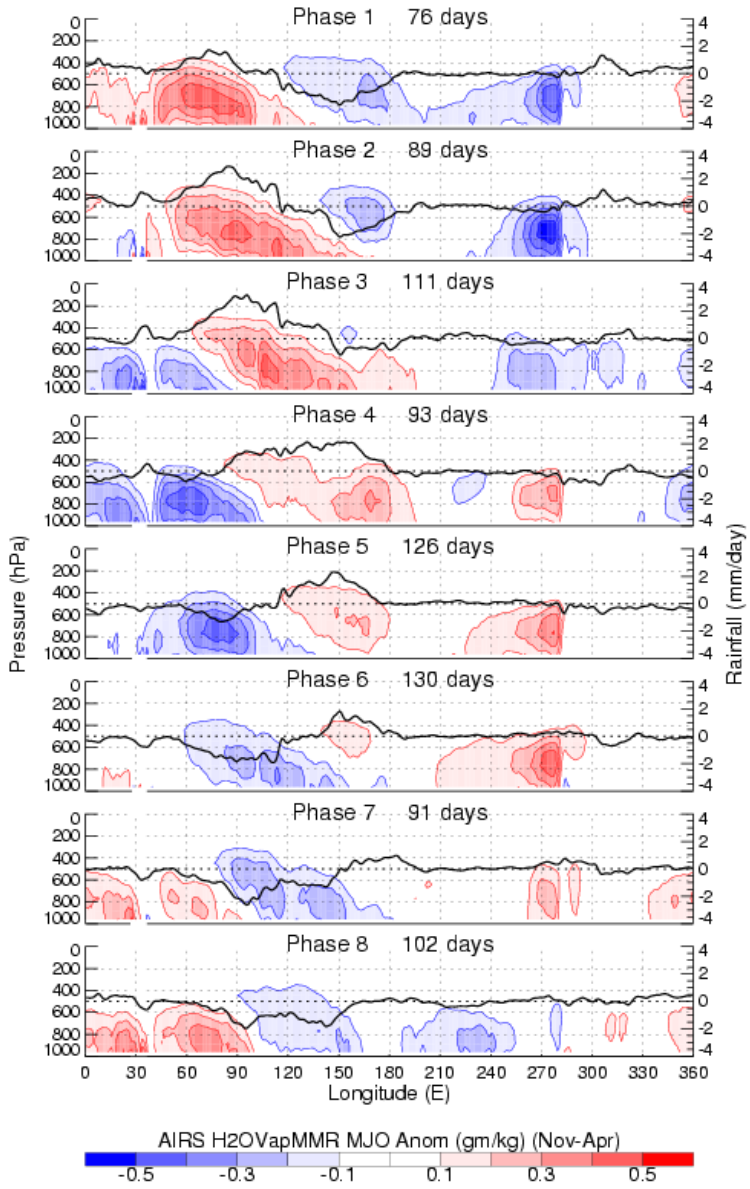

7-yr V5 AIRS data & MEOF method

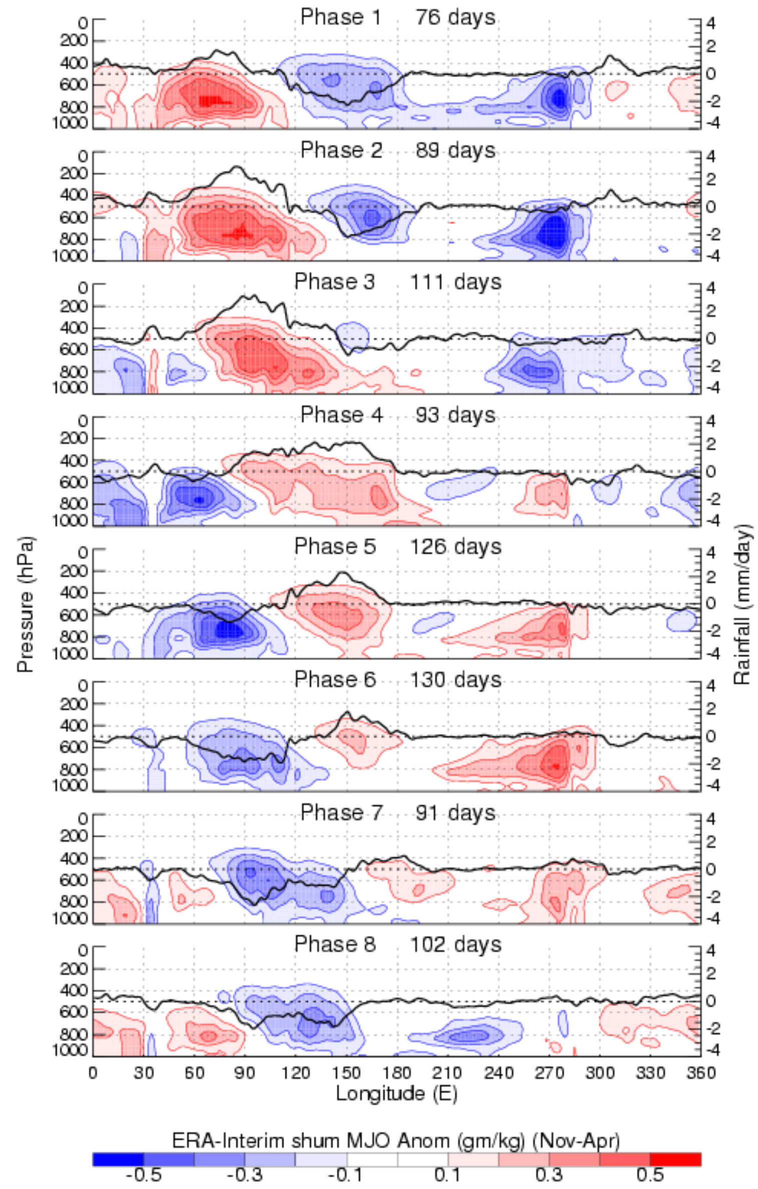

7-yr ERA data & MEOF method

Summary for Part (I)

❖ There is a strong consistency of the large-scale vertical moist thermodynamic structure of the MJO between different AIRS data record lengths (2.5 versus 7 years) and different MJO event selection and compositing methods (the EEOF method used by Tian et al. (2006) versus the MEOF method used by Wheeler and Hendon (2004)).

❖ Deficiencies still exist in the ERA-Interim describing the large-scale vertical moist thermodynamic structure of the MJO although ERA-Interim seems doing much better than NCEP/NCAR in this regard.

Part II

Vertical Cloud Structures of the Boreal Summer Intraseasonal Oscillation Based on CloudSat Observations and ERA-Interim reanalysis

Acknowledgments: Frank Li, and Chris Woods (JPL)

Jiang et al., 2010: *Climate Dynamics*, published on-line.

Rainfall Hovmöller Diagram (75-80°E)

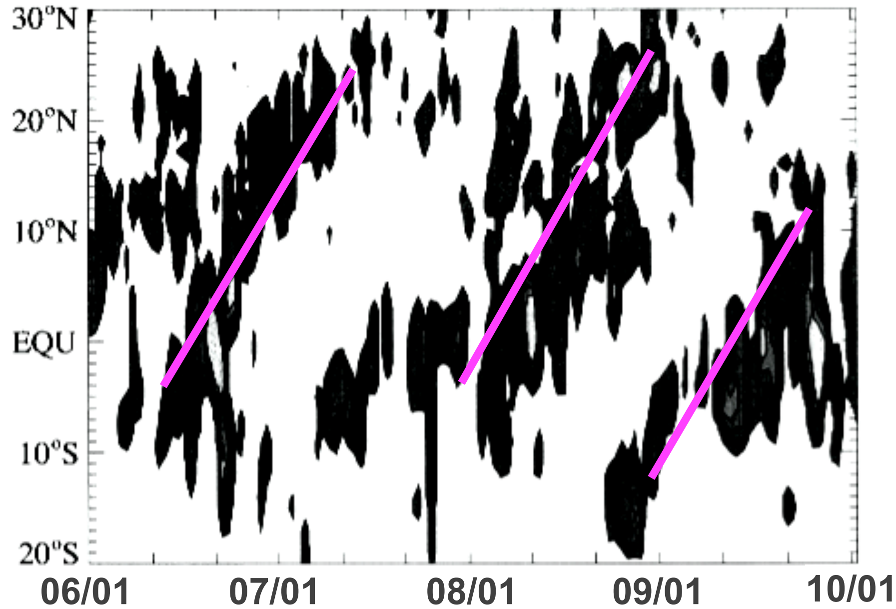

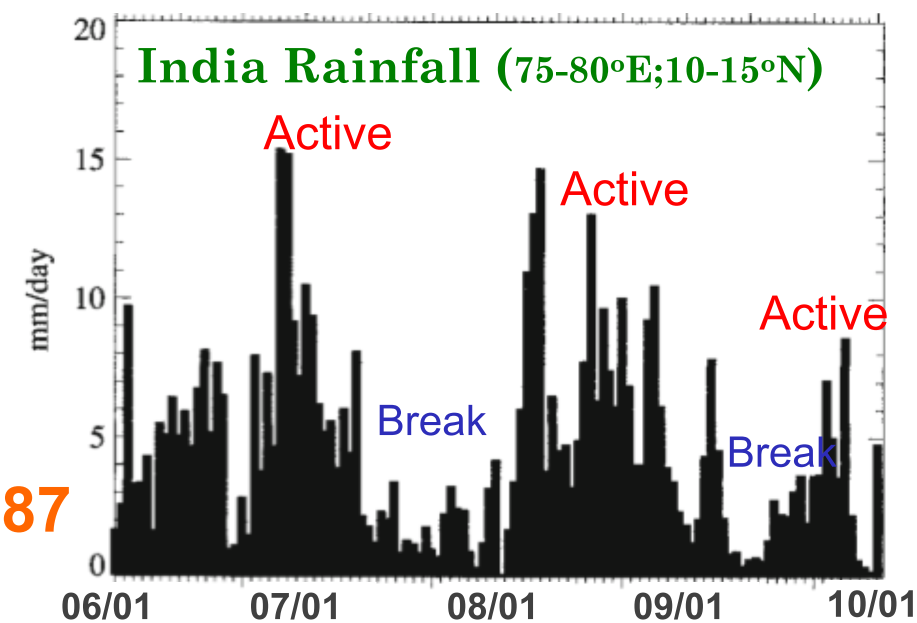

1987

Why the Boreal Summer Intraseasonal Oscillation (BSISO) important?

- Primary source for monsoon predictability;
- Modulate synoptic system activity;

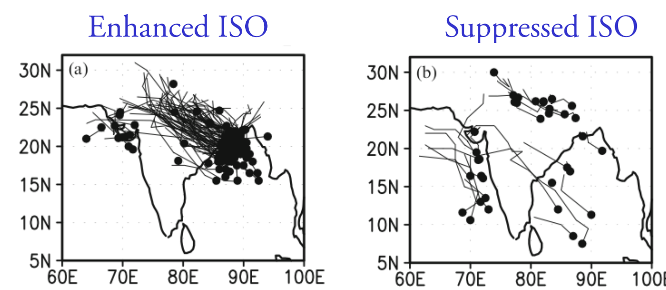

- Affect high/mid-latitude climate through Rossby wave tele-connection.

Lawrence and Webster (2002)

Challenging issues on the BSISO:

- **A perfect theory for the northward propagation of the BSISO, particularly to explain its interannual variability is still elusive;**
- **Current GCMs exhibit limited skills in simulating and predicting the BSISO (Waliser et al., 2003; Kim et al. 2008; Wang 2009).**

CloudSat

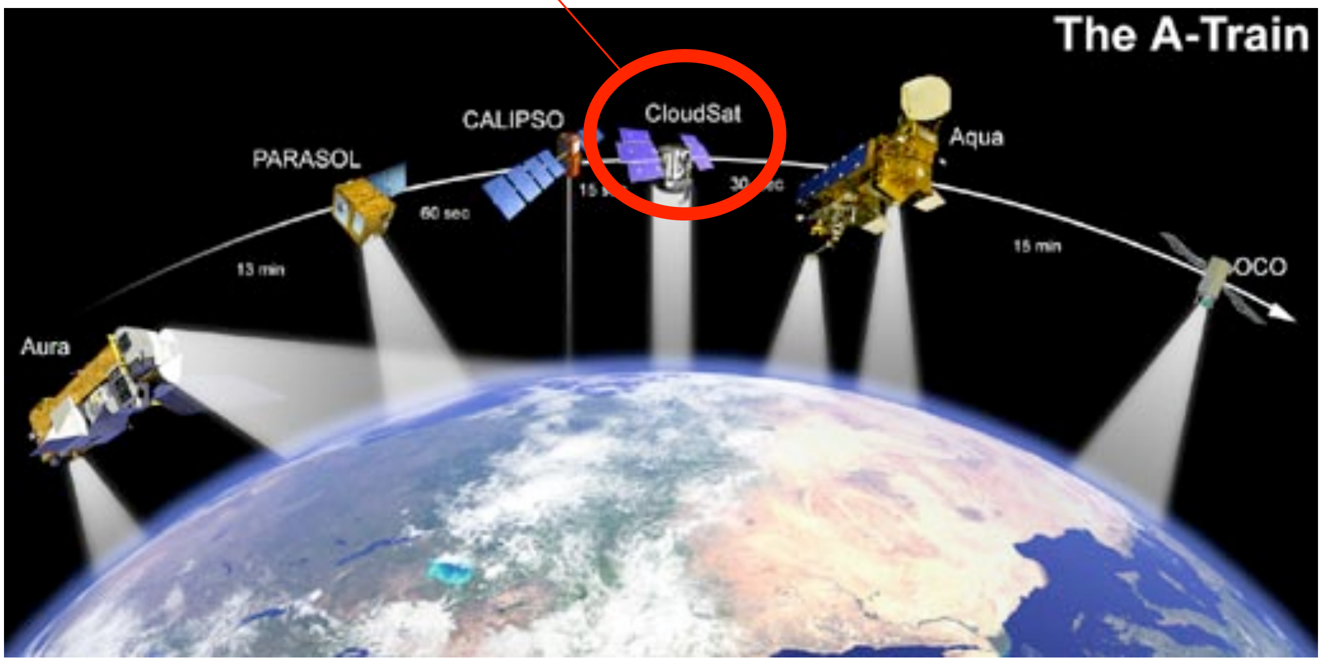

- Launched in April 2006
- Provides a global view of cloud vertical structure
- 94 GHz, nadir-viewing cloud profiling radar
- 1.4 km across-track by 2.5 km along-track footprint
- 500m vertical resolution
- Crossing Equator at 1:31pm

Dataset

CloudSat (Jun– Sep 2006, 2007, 2008)

Horizontal resolution: 1x1 degs, 40 vertical levels between 1025 and 50 hPa

Variables:

Cloud liquid water content (LWC), Ice water content (IWC)

Cloud types (7):

- High: Cirrus
- Middle: Altocumulus (Ac), Altostratus (As)
- Low: Stratocumulus (Sc), Stratus (St), Nimbostratus (Ns)
- Vertical: Cumulus (Cu)

ERA-Interim reanalysis:

Horizontal resolution 1.5 x 1.5 deg, 37 vertical levels

LWC, IWC for Jun-Sep from 2006-2008

TRMM rainfall version 3B42 (1997-2008):

horizontal resolution: 1x1 deg., 20-70-day band-pass filtered

Hovmöller diagram of TRMM precipitation (20-70-day filtered; 75-95^oE)

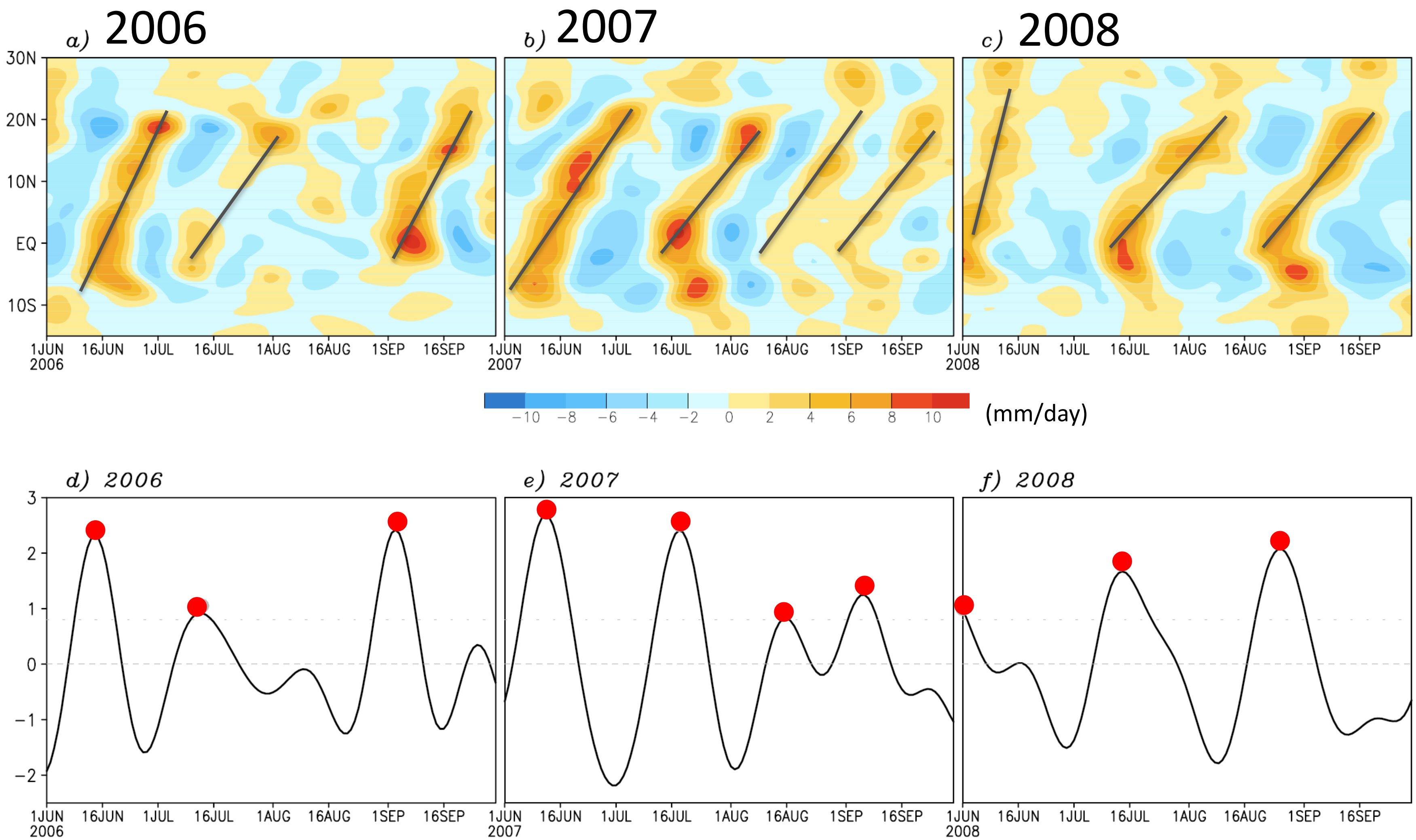

Time series of EEOF1 of daily 1-D 20-70d filtered TRMM rainfall over Indian Sector (5^{o}S~25^{o}N, averaged over 75-95^{o}E sector) for MJJAS, 1996-2008.

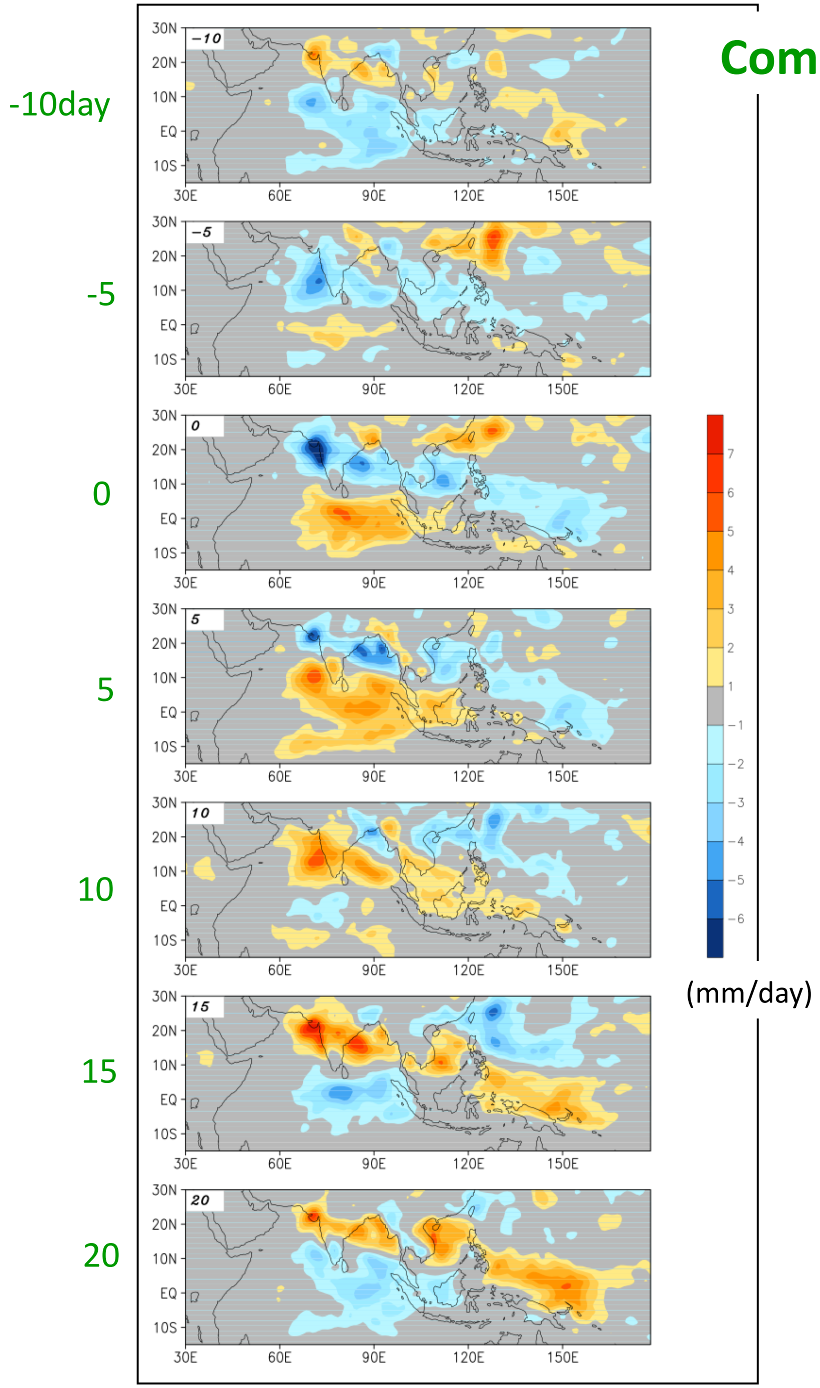

Composite BSISV Evolution (10 events)

TRMM rainfall

Northward propagation

Time-latitude evolution (75-85°E)

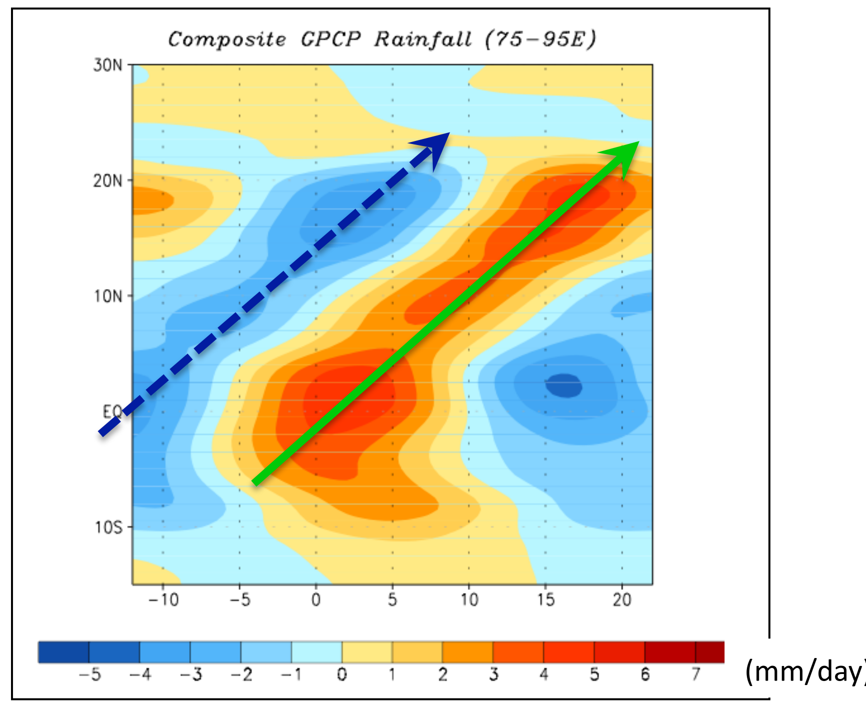

Composite CloudSat LWC (80-95°E average)

(no time-filtering, seasonal mean removed)

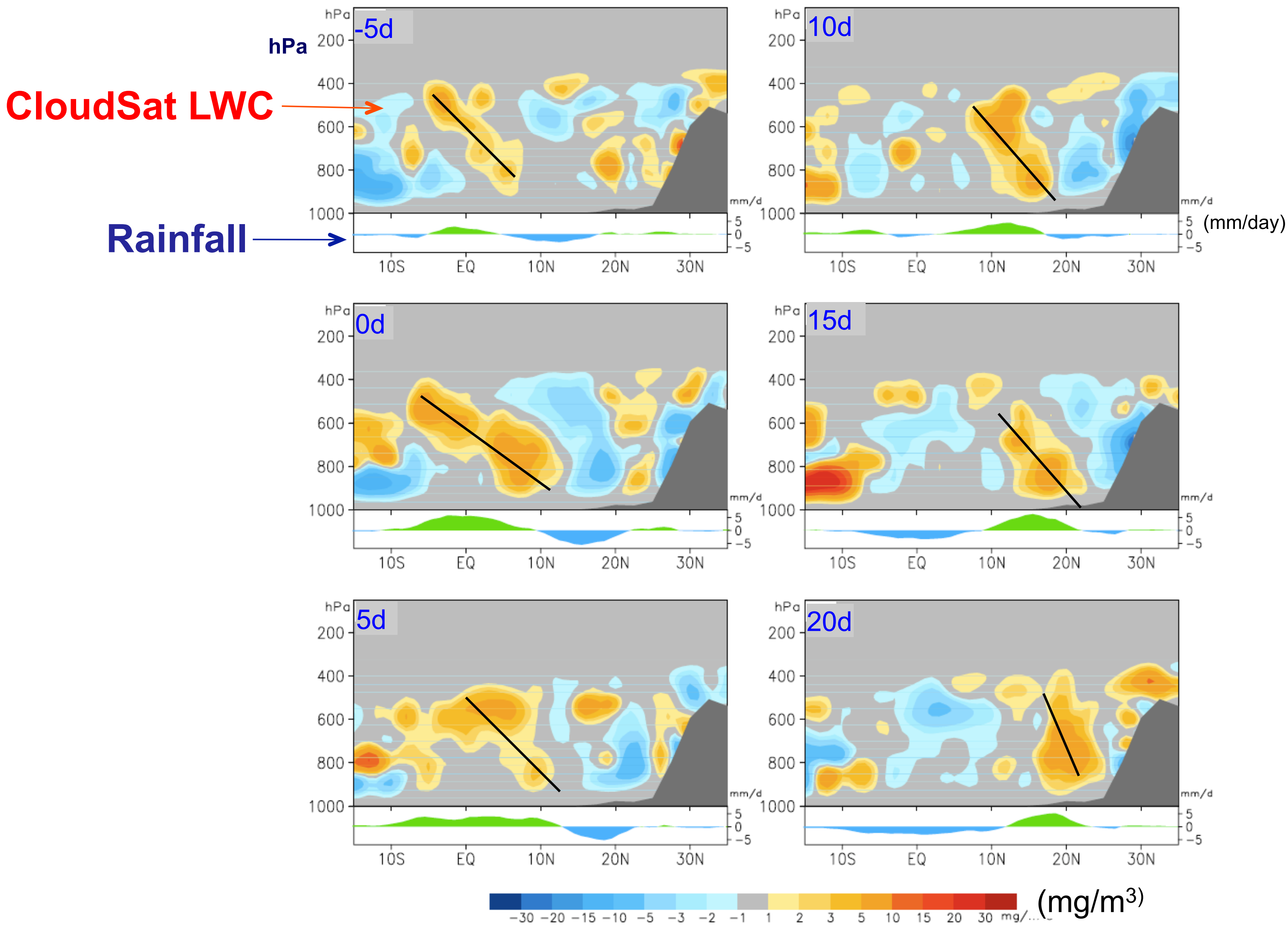

Composite CloudSat IWC (80-95°E average)

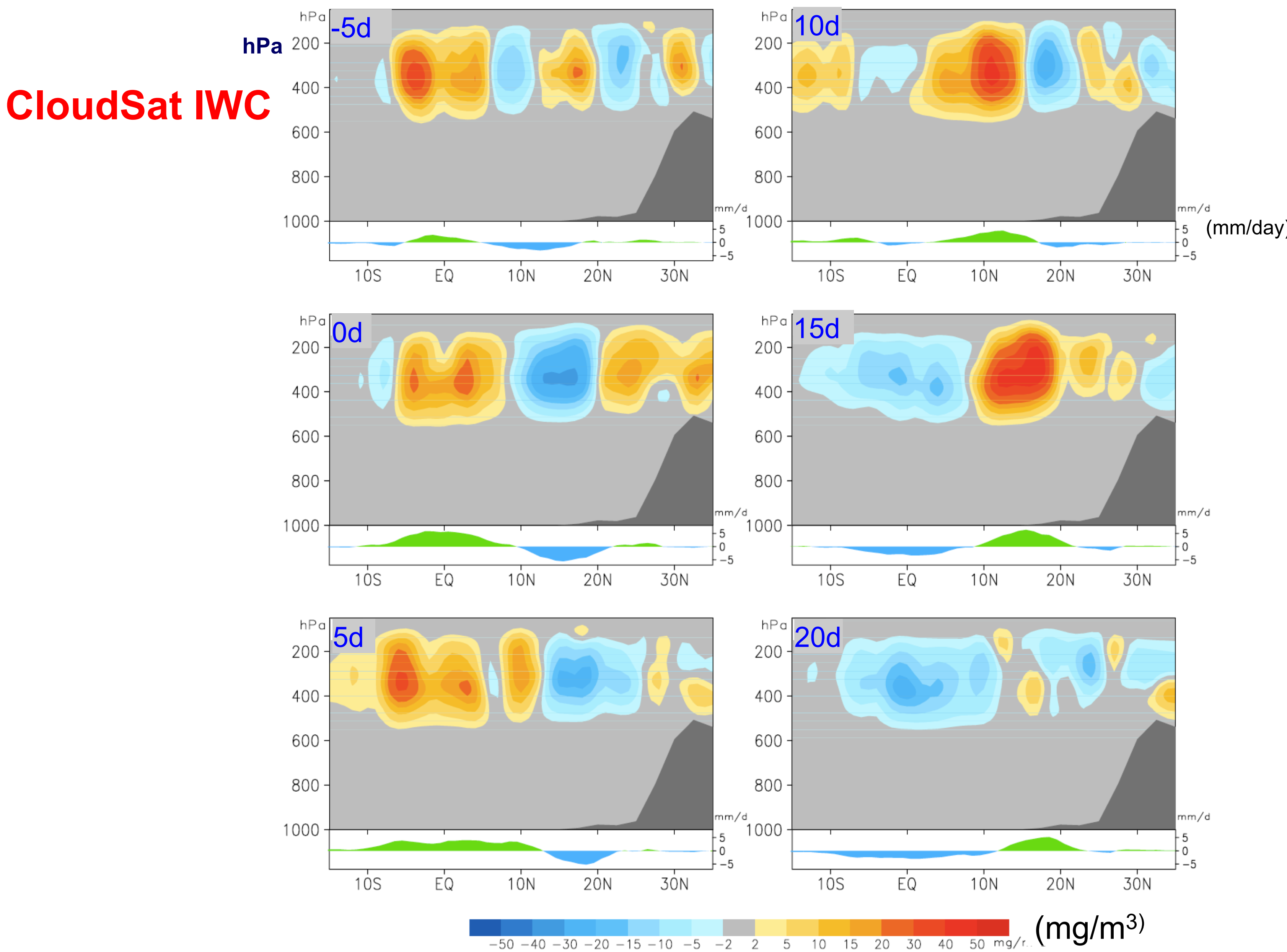

Composite EC-Interim LWC (80-95ºE average)

EC LWC

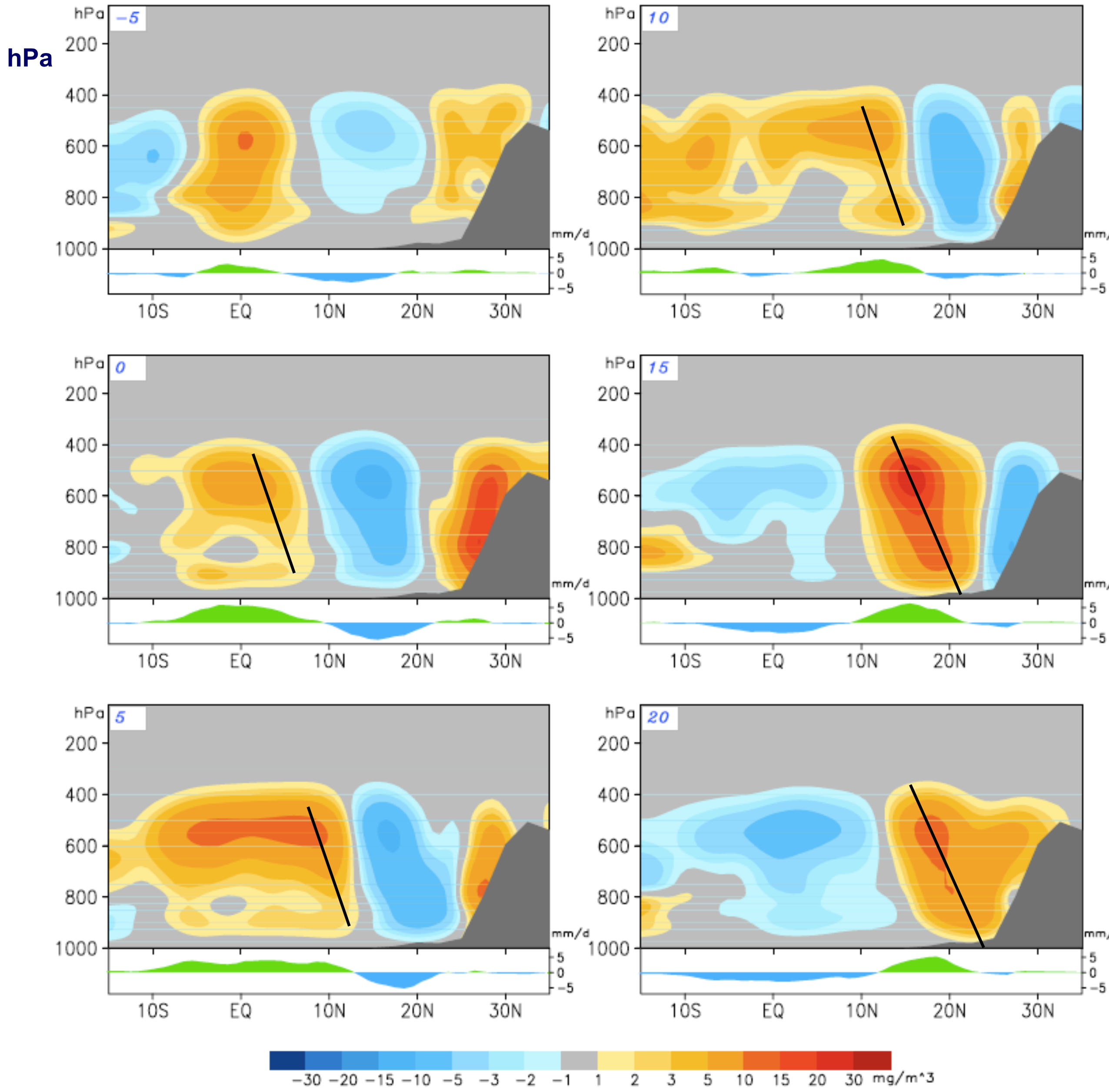

Composite EC-Interim IWC (80-95°E average)

EC IWC

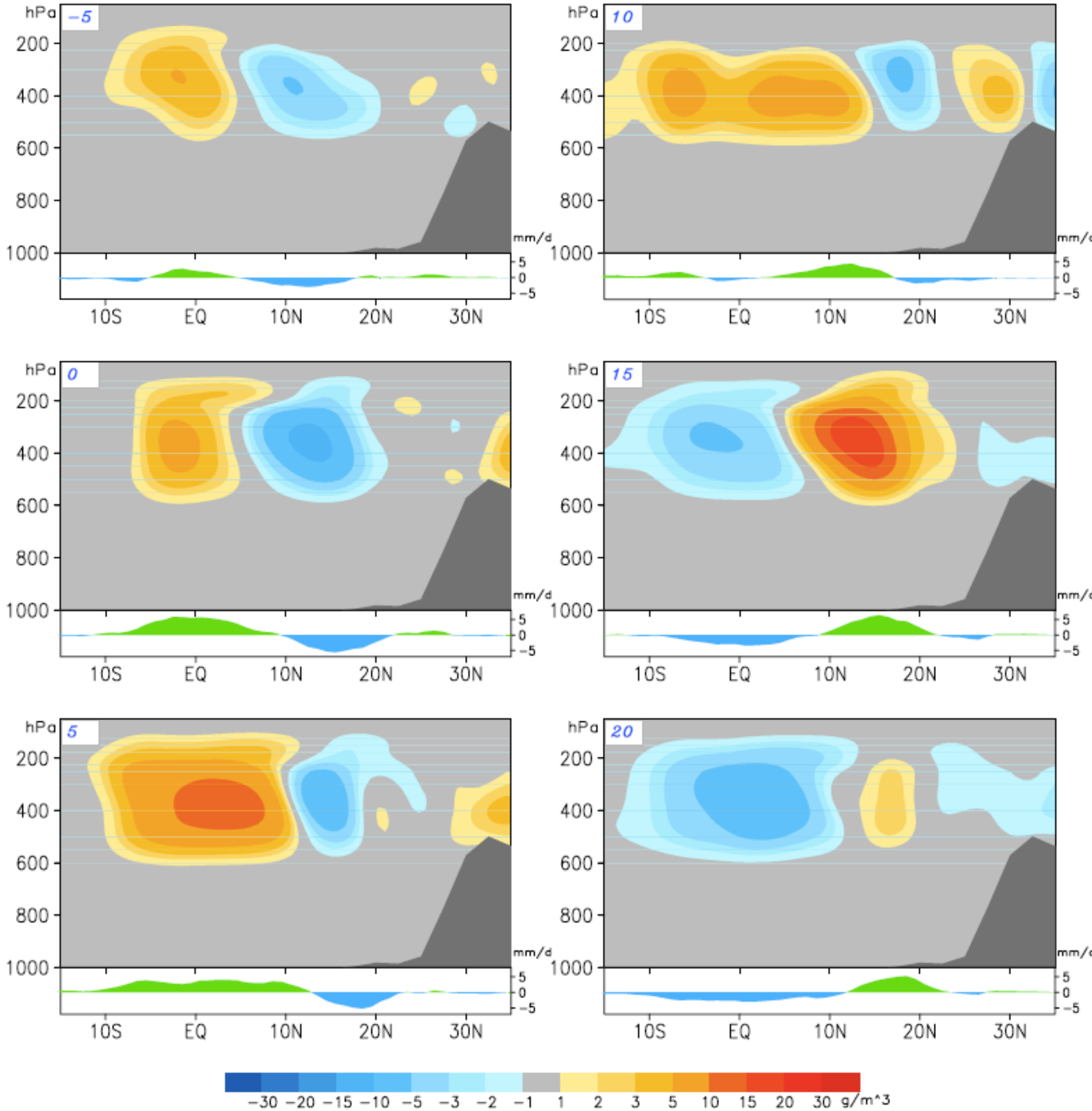

Composite LWC & IWC relative to convection center (mg/m³; 80-95°E)

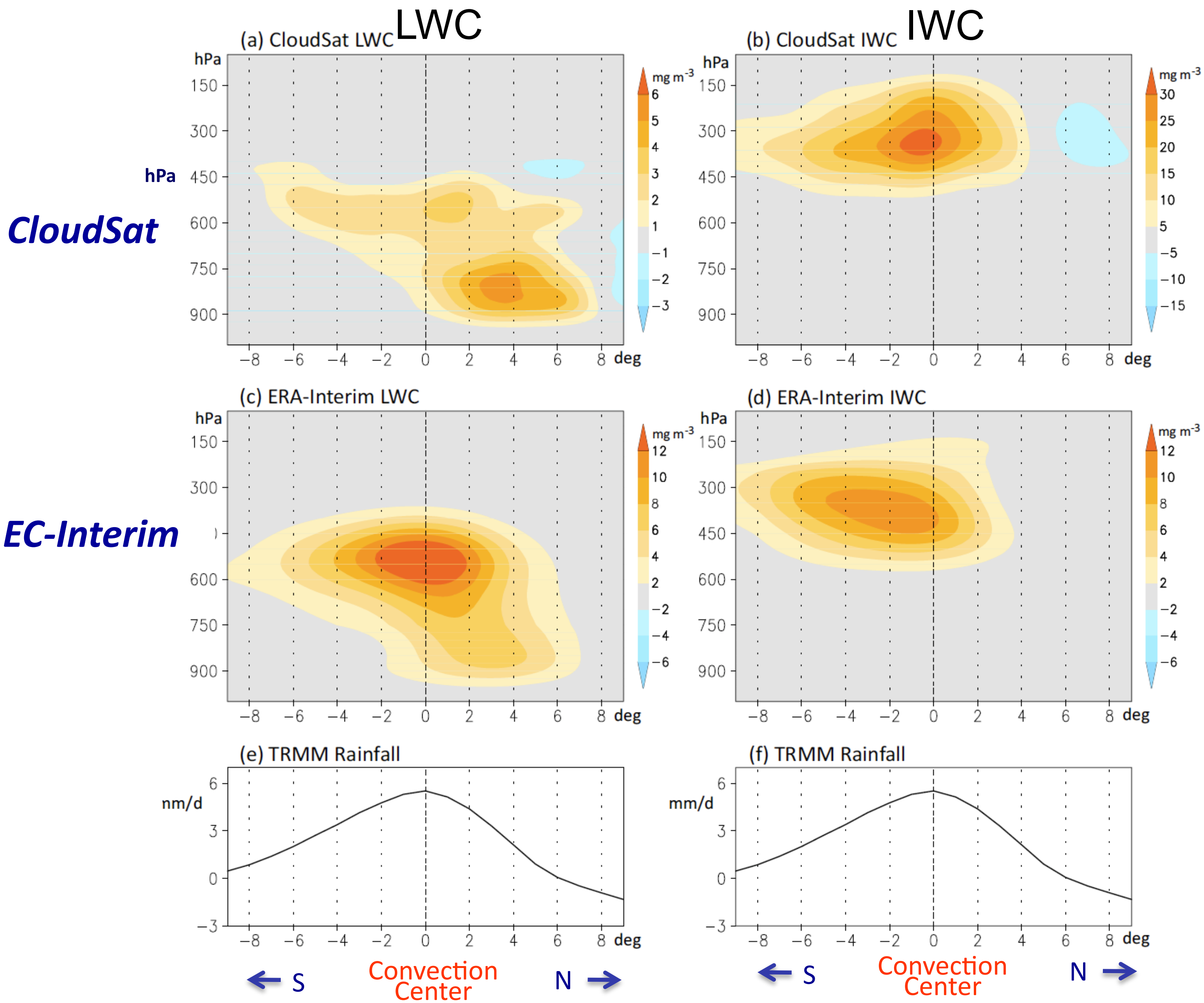

Cloud fraction & circulation associated with the BSISV

CloudSat

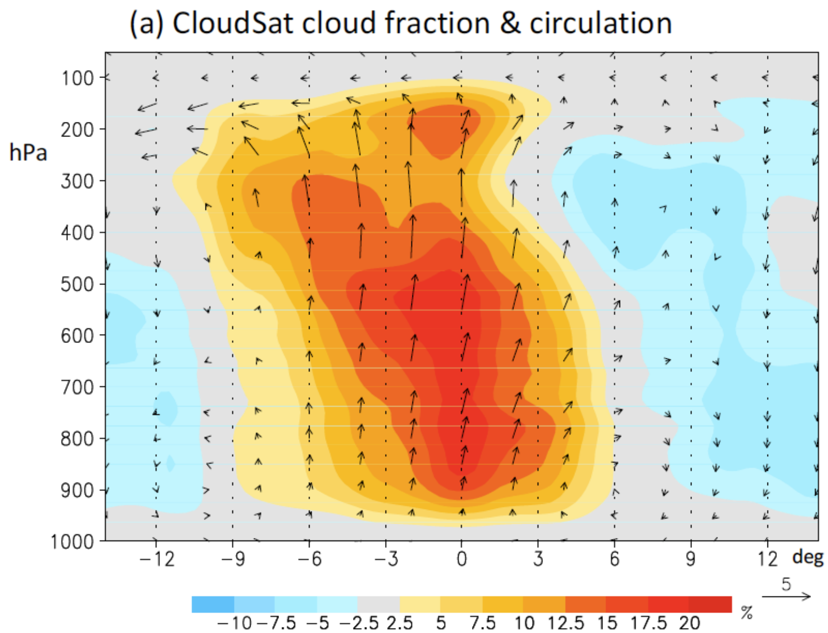

ERA-Interim

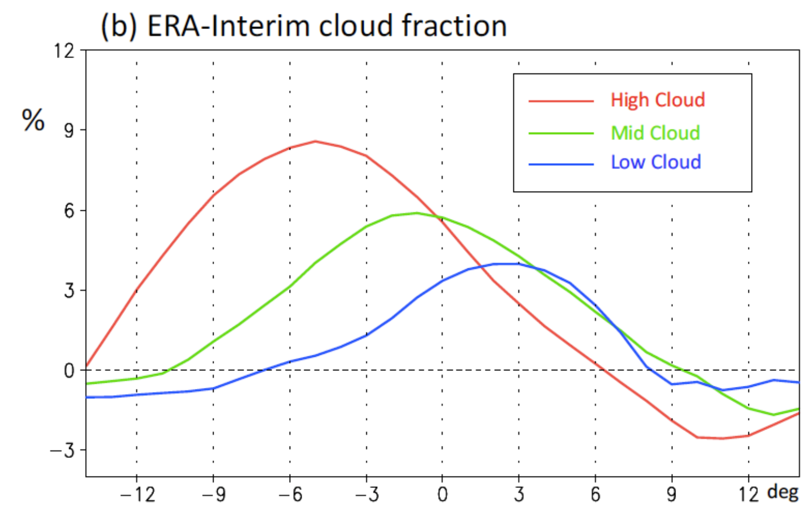

Decompose total cloud fraction by cloud types

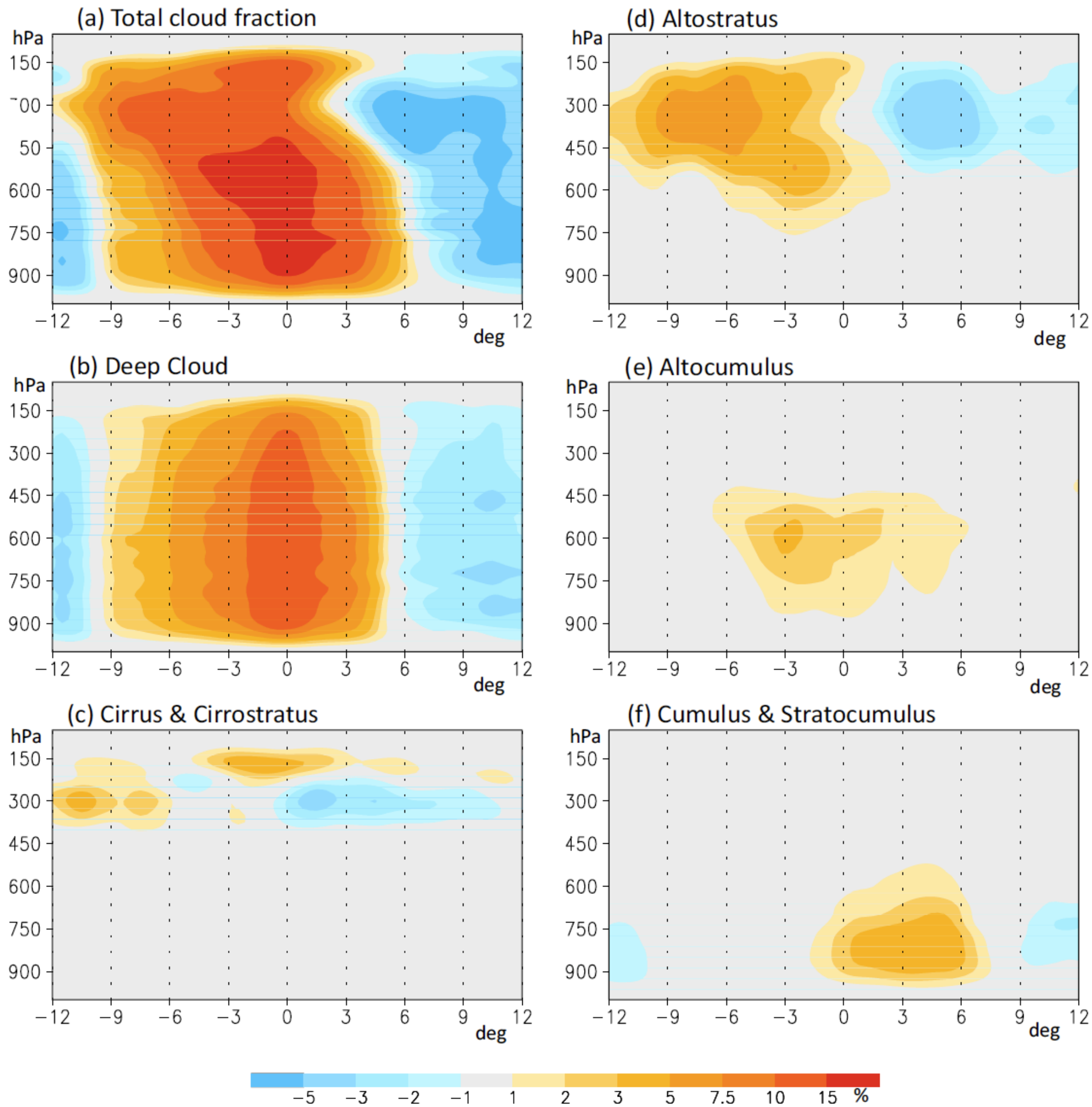

Total Cloud

Deep Convective Cloud

Cirrus

As

Ac

Cu/Sc

Summary for Part (II)

- A marked vertical tilting structure is evident in the cloud liquid water content (LWC) with respect to the convection center of the BSISO based on both CloudSat and ERA-Interim reanalysis.

  Increased LWC tends to appear to the north of rainfall maximum, i.e., leads the convection, particularly in the lower troposphere. This northward shift of increased LWC could be fundamental responsible for the northward propagation of the BSISO.

- The transition in cloud structures associated with BSISV convection is observed based on CloudSat, with shallow cumuli at the leading edge, followed by the deep convective clouds, and then upper anvil clouds.

Caveats

- **Differences in the cloud water content between ERA-Interim reanalysis and the CloudSat observations.**

  Retrieved estimates from CloudSat are expected to also include precipitation sized liquid and ice particles in addition to suspended cloud liquid and ice water content which is the case for the model (e.g., Waliser et al. 2009).

- **Uncertainties involved with the CloudSat estimates, particularly in the low cloud and some of thin cirrus cloud (e.g., Zhang et al. 2007; Terry Kubar, personal communication).**

  Shallow cumulus could be underestimated by CloudSat.

Part III

Vertical Diabatic Heating Structure of the MJO based on TRMM estimates and Reanalysis Datesets

Acknowledgments:

King-Fai Li, Yuk L. Yung /Caltech

TRMM latent heating: Wei-Kuo Tao/GSFC, Bill Olson/UMBC, Shoichi Shige/U. Kyoto

TRMM radiative heating: Tristan L'Ecuyer/CSU

Diabatic heating and MJO theories

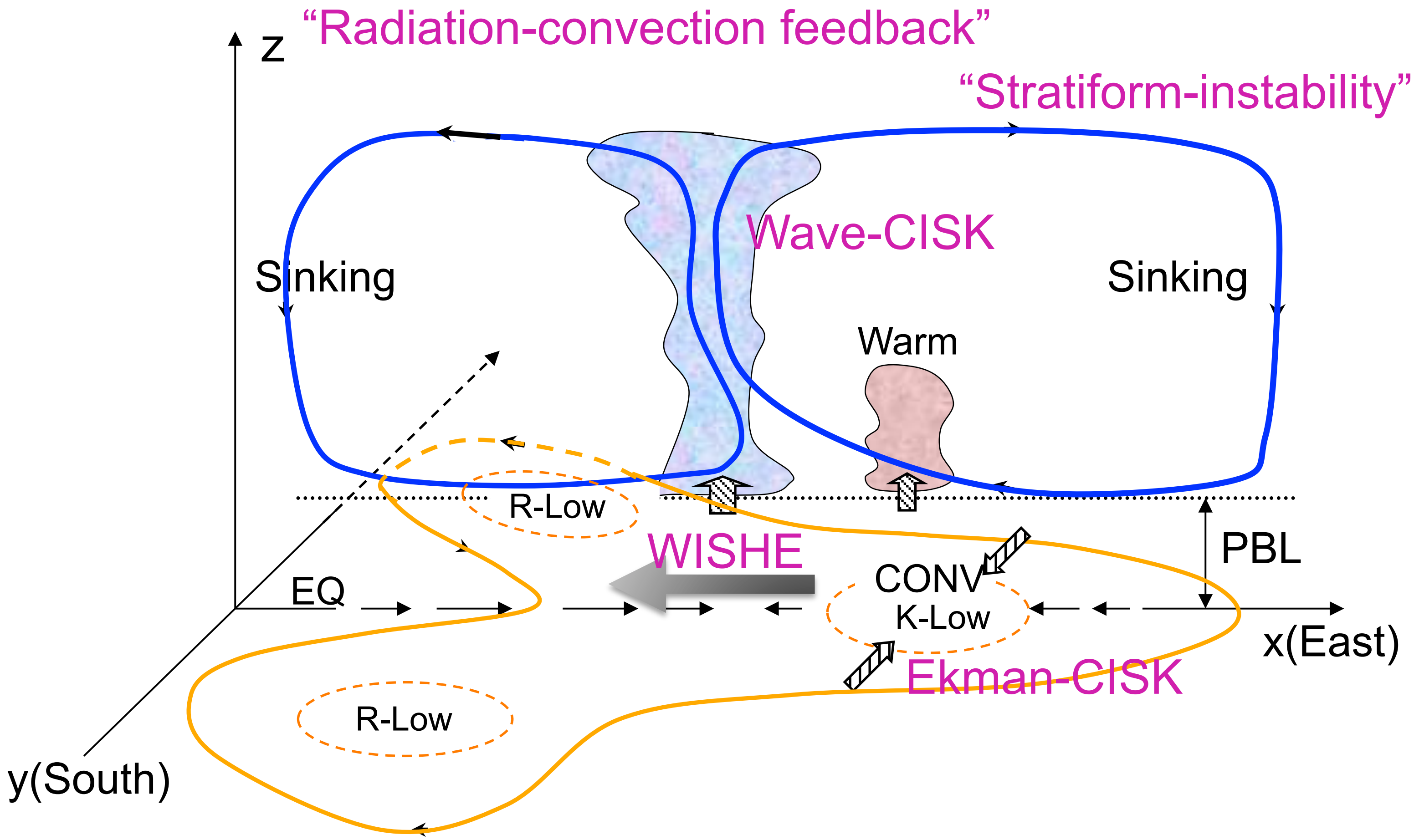

Wang (2005)

“Residual Budget Analysis” Yanai (1973)

$$C_p[\frac{\partial T}{\partial t} + V \cdot \nabla T + w(\frac{RT}{pC_p} - \frac{\partial T}{\partial p})] = Q_1$$

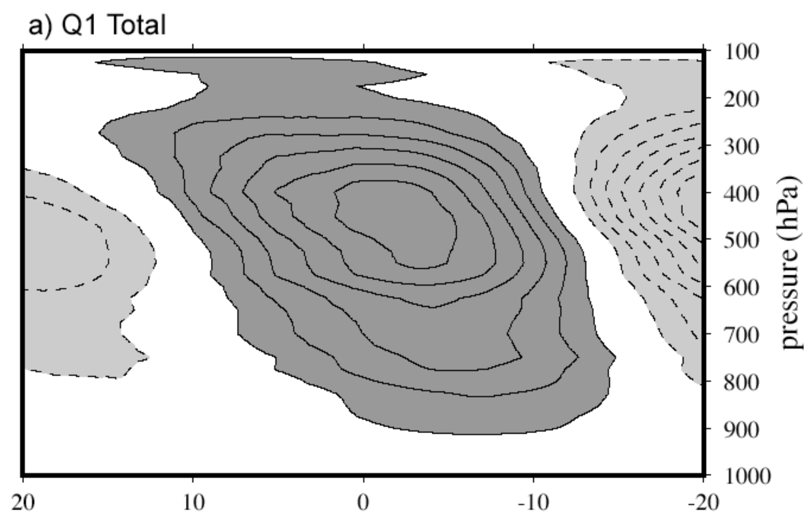

Kiladis et al. 2005

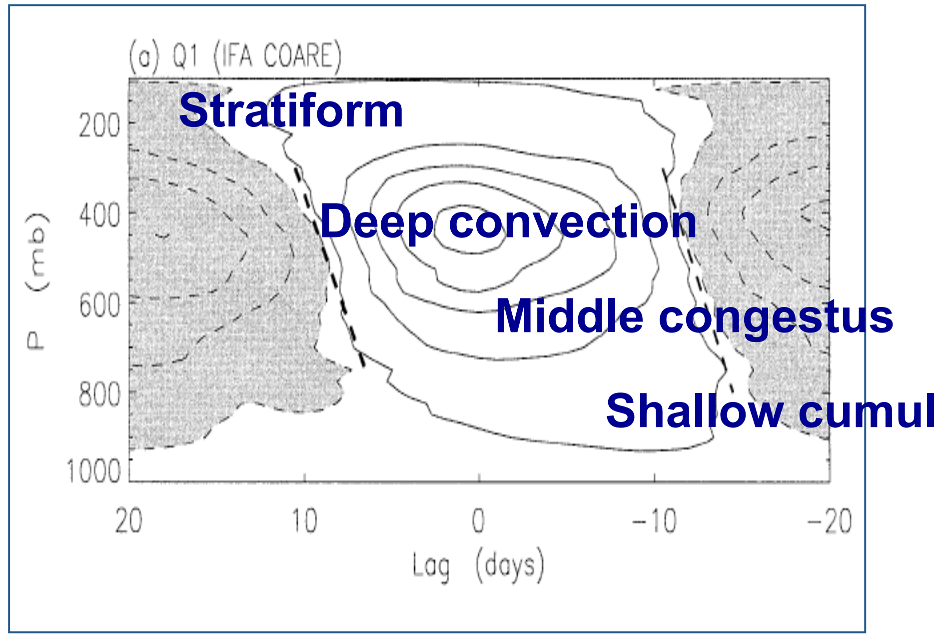

TOGA COARE (10/01/1992~02/28/1993)
sounding array budgets
Lin et al. 2004.

Johnson et al. 1999; Kukuchi and Takayabu 2004; Kiladis et al 2005; Schumacher et al. 2007; and others.

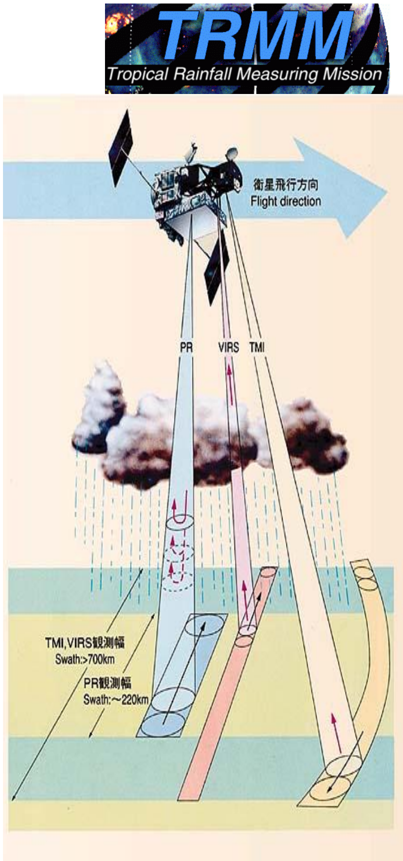

Tao et al. (2006), BAMS

RETRIEVAL OF LATENT HEATING FROM TRMM MEASUREMENTS

BY W.-K. TAO, E. A. SMITH, R. F. ADLER, Z. S. HADDAD, A. Y. HOU, T. IGUCHI, R. KAKAR, T. N. KRISHNAMURTI, C. D. KUMMEROW, S. LANG, R. MENEGHINI, K. NAKAMURA, T. NAKAZAWA, K. OKAMOTO, W. S. OLSON, S. SATOH, S. SHIGE, J. SIMPSON, Y. TAKAYABU, G. J. TRIPOLI, AND S. YANG

TRMM-based latent heating products—not long ago considered out of our technological reach—are beginning to contribute to global modeling, but the necessary retrieval algorithms produce varying results and will require further research.

$$Q_1 = \underbrace{\frac{L_v}{c_p}(\bar{c}-\bar{e}) + \frac{L_f}{c_p}(\bar{f}-\bar{m}) + \frac{L_s}{c_p}(\bar{d}-\bar{s})}_{\text{phase change or “latent heating”}} + \underbrace{\bar{\pi}\left(-\overline{V'\bullet\nabla\theta'} - \frac{1}{\bar{\rho}}\frac{\partial\bar{\rho}\overline{w'\theta'}}{dz}\right)}_{\text{eddy sensible heat flux convergence}} + \underbrace{Q_R}_{\text{radiative heating}}$$

Dataset and approach:

TRMM Q_1 estimates

Olson/Grecu*:* TMI-Based "TRAIN" Estimates

Tao/Lang*:* PR -Based "CSH" Algorithm

Shige: PR -Based "SLH" Algorithm

TRMM Q_R estimates: L'Ecuyer (Q_R)

Reanalysis datasets:

ERA -Interim (Residual Budget Approach derived; u, v, w, T);

NASA MERRA (Direct model output);

NCEP CFS-R (Direct model output);

Period: 1998-2008

Composite Approach: Wheeler and Hendon RMM_1, RMM_2 index
Amplitudes >= 1 for November to December.

Q_1 (10S-10N)

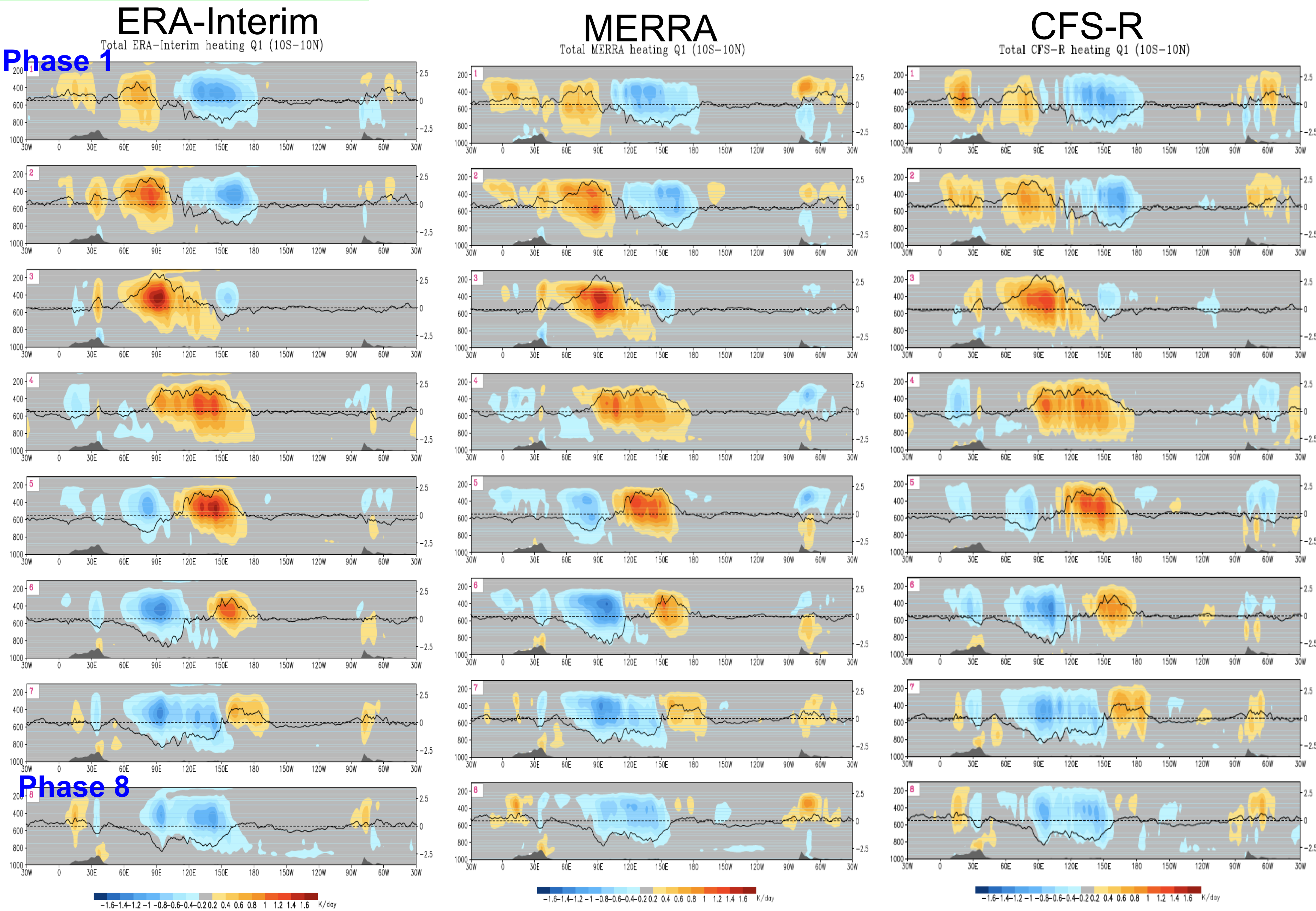
ERA-Interim
Total ERA-Interim heating Q1 (10S-10N)
MERRA
Total MERRA heating Q1 (10S-10N)
CFS-R
Total CFS-R heating Q1 (10S-10N)
Phase 1
Phase 8
30W 0 30E 60E 90E 120E 150E 180 150W 120W 90W 60W 30W
200 400 600 800 1000
2.5 0 -2.5
-1.6 -1.4 -1.2 -1 -0.8 -0.6 -0.4 -0.2 0.2 0.4 0.6 0.8 1 1.2 1.4 1.6 K/day

Q_1 (10S-10N)

TRAIN

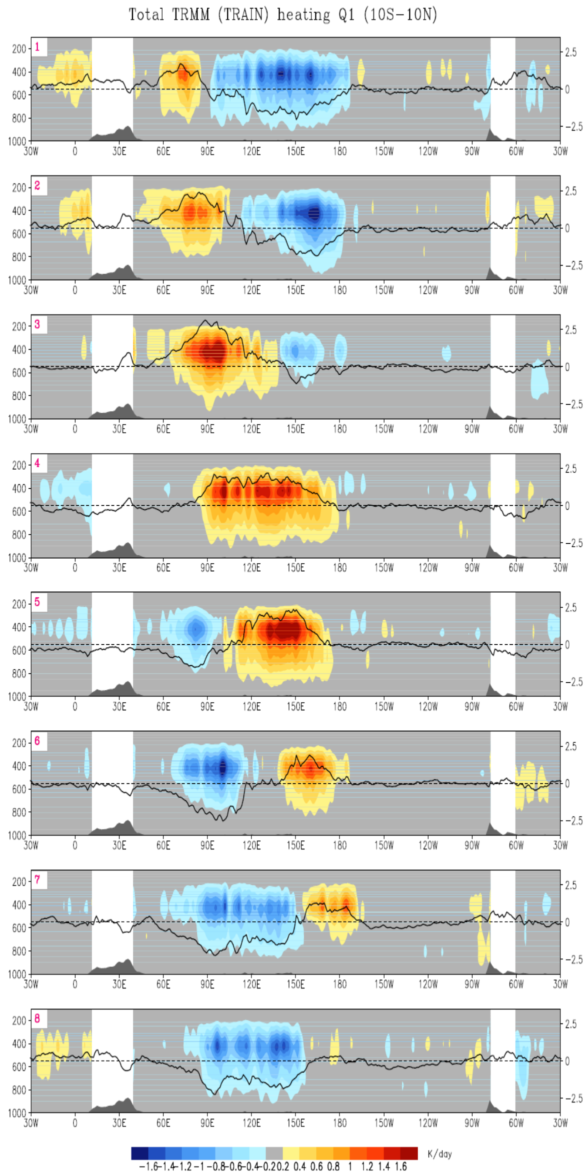

SLH

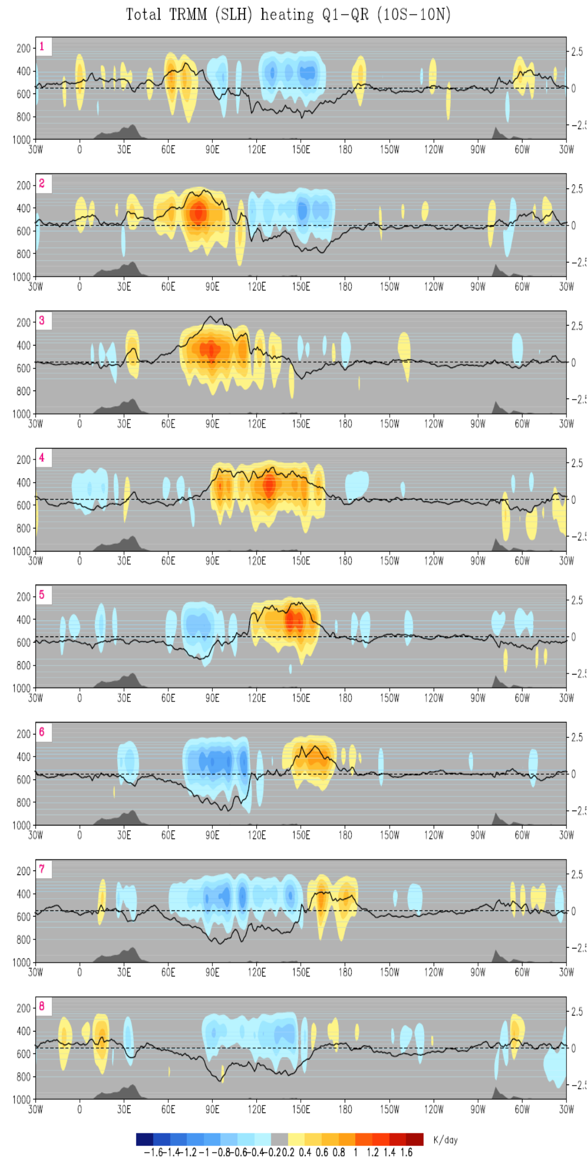

CSH

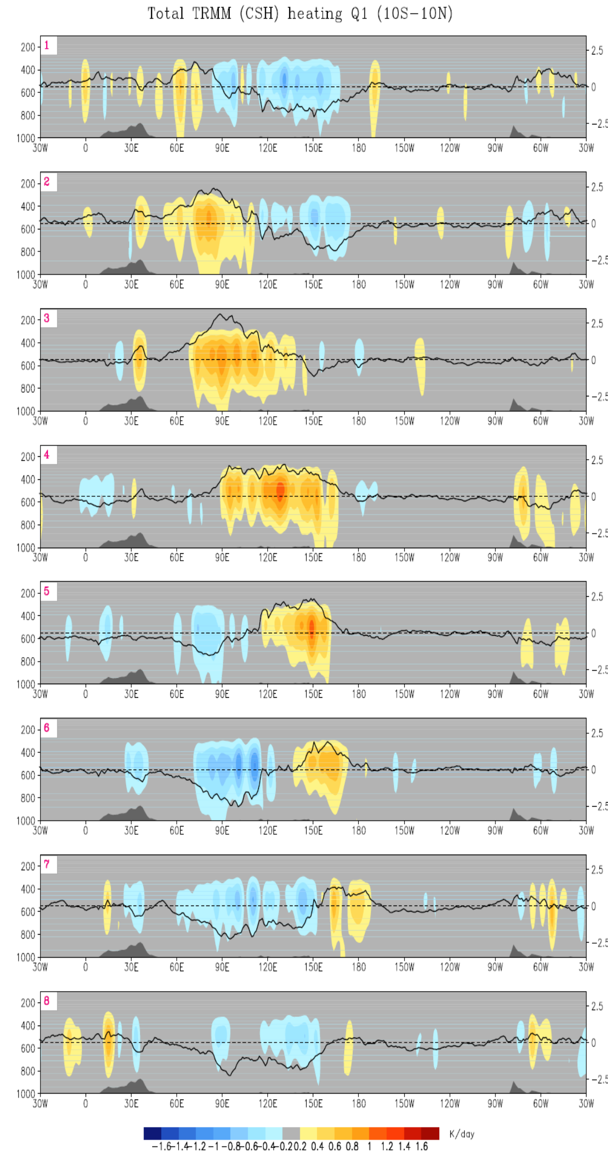

Q_1 (150-160°E; 10°S-10°N; ~ TOGA-COARE)

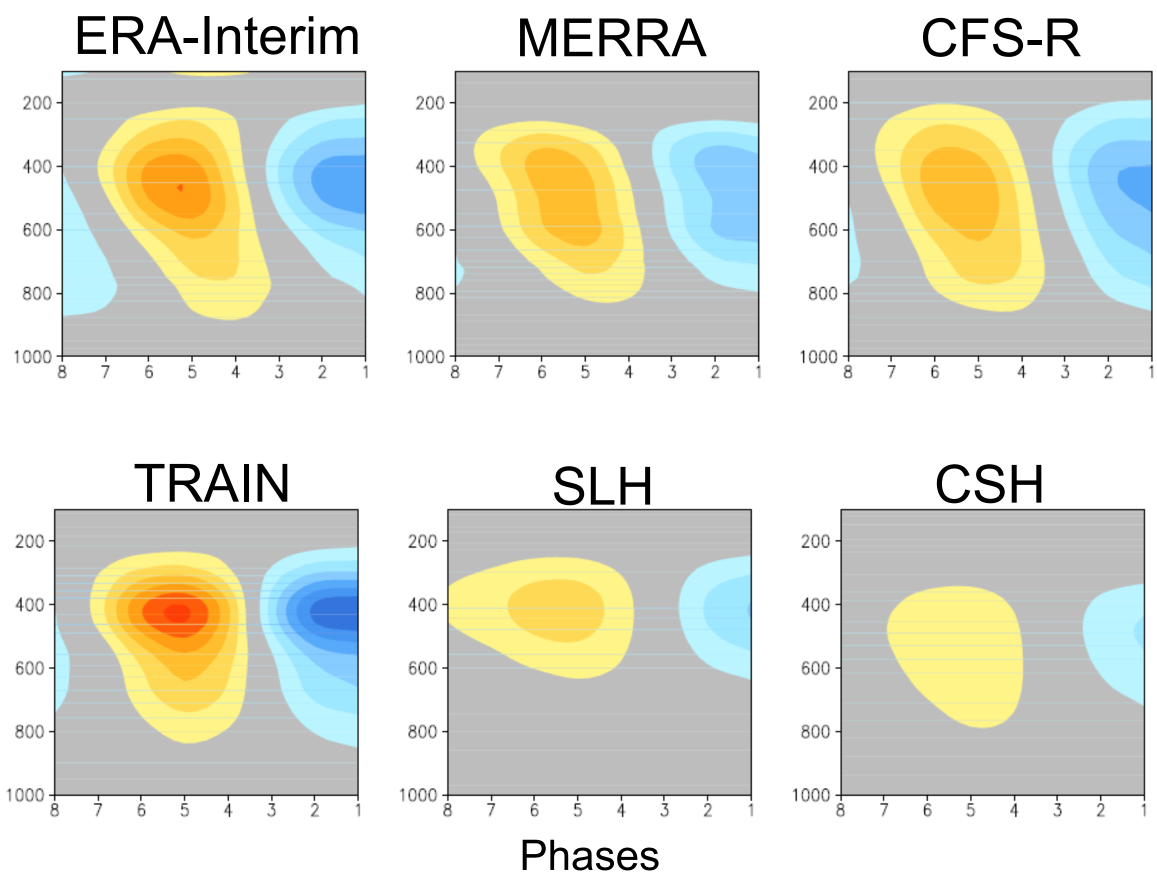

Lin et al. 2004
(TOGA-COARE)

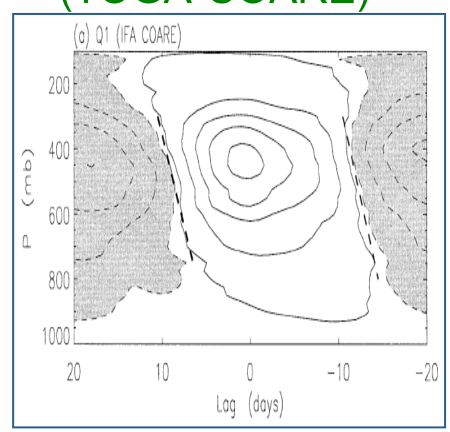

Caveats

TRMM algorithm:

- Look-up table for TRMM estimates heavily depends on CRM which is subject to parameterization in microphysics.

Reanalyses:

- Model responses to large-scale dynamical/thermo-dynamical forcing by cumulus parameterization module.

- Need to understand satellite vs. reanalysis differences in terms of water vapor & cloud differences.